Analogues of Cis- and Transplatin with a Rich Solution Chemistry: *cis*-[PtCl$_2$(NH$_3$)(1-MeC-*N3*)] and *trans*-[PtI$_2$(NH$_3$)(1-MeC-*N3*)]**

Sabine Siebel, Claudia Dammann,[b] Pablo J. Sanz Miguel,[c] Thomas Drewello,[b] Gunnar Kampf,[a] Natascha Teubner,[a] Patrick J. Bednarski,[d] Eva Freisinger,[e] and Bernhard Lippert*[a]

[a] Dr. S. Siebel, Dr. G. Kampf, N. Teubner, Prof. Dr. B. Lippert. Fakultät Chemie und Chemische Biologie (CCB), Technische Universität Dortmund, Otto-Hahn-Str. 6, 44221 Dortmund (Germany). Fax: (+49) 231-755-3797. E-mail: bernhard.lippert@tu-dortmund.de

[b] C. Dammann, Prof. Dr. T. Drewello. Physikalische Chemie I, Universität Erlangen-Nürnberg, Egerlandstrasse 3, 91058 Erlangen (Germany).

[c] Dr. P. J. Sanz Miguel. Departamento de Química Inorgánica, Instituto de Síntesis Química y Catálisis Homogèna (ISQCH), Universidad de Zaragoza-CSIC, 50009 Zaragoza, Spain

[d] Prof. Dr. P. J. Bednarski. Pharmazeutische/Medizinische Chemie, Institut für Pharmazie der Ernst-Arndt-Universität Greifswald, Friedrich-Ludwig-Jahn-Straße 17, 17487 Greifswald (Germany)

[e] Priv.-Doz. Dr. E. Freisinger. Department of Chemistry, University of Zürich, Winterthurerstrasse 190, 8057 Zürich (Switzerland)

(1-MeC = 1-Methylcytosine)

Dedicated to Professor Giovanni Natile on the occasion of his 70th birthday

ABSTRACT

Mono(nucleobase) complexes of general composition *cis*-PtCl$_2$(NH$_3$)L with L = 1-methylcytosine, 1-MeC (**1a**) and L = 1-ethyl-5-methylcytosine, as well as *trans*-[PtX$_2$(NH$_3$)(1-MeC)] with X = I (**5a**) and X = Br (**5b**), have been isolated and were characterized by X-ray crystallography. The Pt coordination occurs through N3 atom of the cytosine in all cases. The diaqua complexes of compounds **1a** and **5a**, *cis*-[Pt(H$_2$O)$_2$(NH$_3$)(1-MeC)]$^{2+}$ and *trans*-[Pt(H$_2$O)$_2$(NH$_3$)(1-MeC)]$^{2+}$ display a rich chemistry in aqueous solution, which is dominated by extensive reactions leading to µ-OH and µ-(1-MeC$^-$-*N3,N4*) bridged species and ready oxidation of Pt to mixed-valence state complexes as well as diplatinum(III) compounds, one of which was characterized by X-ray crystallography: *h,t*-[{Pt(NH$_3$)$_2$(OH)(1-MeC$^-$-*N3,N4*)}$_2$](NO$_3$)$_2$·2[NH$_4$](NO$_3$)·2H$_2$O. A combination of ^{1}H NMR spectroscopy and ESI mass spectrometry was applied to identify some of the various species present in solution and the gas phase, respectively. As it turned out, mass spectrometry did not permit an unambiguous assignment of the structures of +1 cations due to the possibilities of realizing multiple bridging patterns in isomeric species, the occurrence of different tautomers, and uncertainties regarding the Pt oxidation states. Additionally, compound **1a** was found to have selective and moderate antiproliferative activity for a human cervix cancer line (SISO) compared to six other human cancer cell lines.

Introduction

Among the great surprises research on antitumor–active Pt coordination compounds has provided over the past decades are findings, that most of the "rules of thumb" regarding the activity of Pt complexes, coined during the early days of work on the structure-activity relationships of cisplatin,[1] found their exceptions.[2] Cases include the following examples: i) Substitution of one of the two ammonia ligands of Cisplatin by a N-heterocyclic ligand without any hydrogen bond donor ability can retain its activity. Picoplatin, in which 2-2-methylpyridydine (2-picoline) replaces a NH_3 ligand, is a prime example.[3] ii) Even the corresponding *trans*-isomer displays activity against cancer cell lines,[4] despite the fact that the *trans* isomer of cisplatin, that is, *trans*-[PtCl$_2$(NH$_3$)$_2$], is hardly active. iii) Substitution of a chlorido ligand of cisplatin (or structural analogues) by N-heterocyclic ligands L,[5] which generates cationic and monofunctional Pt species of general formula *cis*-[PtCl(NH$_3$)$_2$(L)]$^+$ also leads to active compounds. Interestingly, the first complex of this type showing antitumor activity, contained the pyrimidine parent nucleobase cytosine.[5a,5b] A related example, with the two ammonia ligands replaced by a chelating 2,9-dimethyl-1,10-phenanthroline ligand, chloride by iodide, and L being the model nucleobase 1-methylcytosine, was later reported to have a distinctly different mode of action than cisplatin and to overcome Cisplatin resistance.[5d]

Reasons for these "exceptions" probably are diverse: Thus, it has been proposed that the activity of picoplatin is the consequence of an altered, namely slowed-down hydrolytic activation of the Pt drug due to steric crowding about the Pt center as caused by the *ortho* substituent of the pyridine ligand,[6] and the activity of the cationic [PtCl(NH$_3$)$_2$(L)]$^+$ has been attributed to its unique monofunctional coordination pattern to the putative DNA target molecule.[7]

Our interest in studying complexes of types i) and ii) and their hydrolyzed derivatives, respectively, with the N-heterocycle being 1-methylcytosine (1-MeC) originated, apart from the feasibility to have active compounds in hands, from our wish to obtain a deeper understanding of acid-base properties of Pt-aqua groups in dependence of the microenvironment,[8] and to extend our knowledge on condensation patterns leading to higher nuclearity clusters.[9] Compounds of type iii) finally have been widely applied by us as precursors for the preparation of models of cisplatin–DNA adducts with two identical or different nucleobases[10] or even tris(nucleobase) adducts.[11] Figure 1 lists the three groups of active Pt complexes i)–iii) derived from cisplatin and its *trans* isomer, as well as the two 1-MeC complexes studied in this paper.
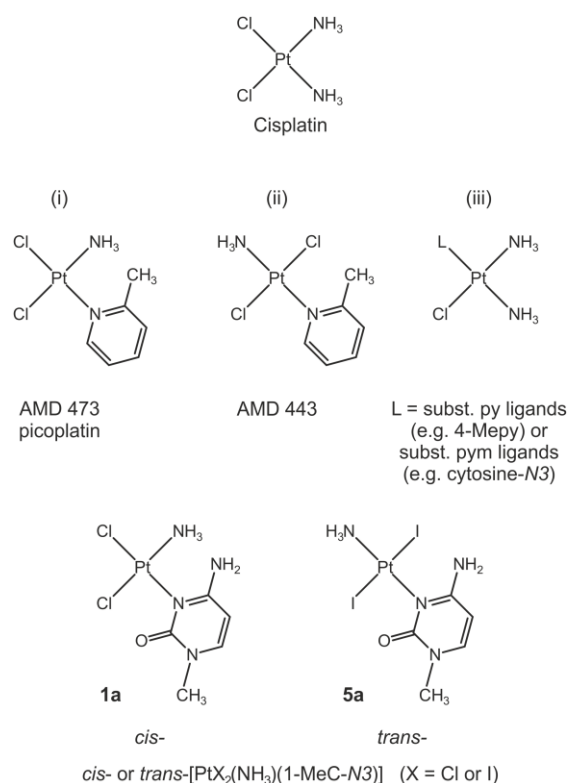

Figure 1. Cisplatin (top), active complexes with single N-heterocyclic ligands (middle), and 1-methylcytosine (1-MeC) compounds (bottom) studied in this work.

Results and Discussion

cis-[PtCl$_2$(NH$_3$)(1-MeC-*N3*)] (1a) and *cis*-[PtCl$_2$(NH$_3$)(1-Et-5-MeC-*N3*)]·H$_2$O (1b)

The two compounds **1a** and **1b** were prepared by treating [PtCl$_3$(NH$_3$)]$^-$ with 1-MeC and 1-Et-5-MeC, respectively, in the presence of excess NaCl. NaCl was applied in order to avoid further reaction to bis- and tris-cytosine complexes. Only compound **1a** could be isolated in good yield, but both components were characterized by X-ray crystallography. Figure 2 provides views of compounds **1a** and **1b**.
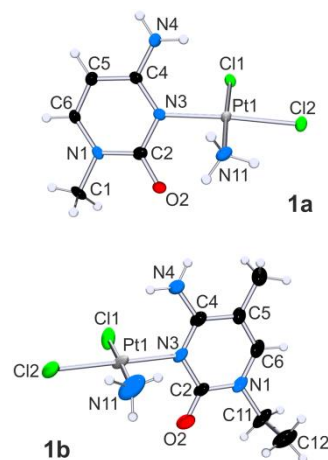

Figure 2. Views of complexes **1a** and **1b** with atom numbering schemes. Ellipsoids are drawn at the 30% probability level.

Due to the asymmetry of the cytosine ligands both complexes are chiral. Salient structural features (for more data, see Table S1 in the Supporting Information) are as follows: Pt1–N3, 2.047(4) Å (**1a**), 2.034(5) Å (**1b**); Pt1–N11(NH$_3$), 2.030(5) Å (**1a**), 2.004(6) Å (**1b**); Pt1–Cl1, 2.3027(14) Å (**1a**), 2.3134(18) Å (**1b**); Pt1–Cl2, 2.2899(12) Å (**1a**), 2.2933(16) Å (**1b**); dihedral angle cytosine plane/Pt plane, 66.83(11)° (**1a**), 76.80(14)° (**1b**). As can be seen, there is a trend that Pt1–Cl1 bonds, hence those *trans* to NH$_3$ are longer than the Pt1–Cl2 bonds, and at least for **1a**, this difference is significant (9σ), consistent with findings for the 2-picoline and 3-picoline analogues.[6] It suggests a higher *trans* influence of NH$_3$ over the N3-bound cytosine nucleobase.

Diaqua species of compound 1a

Types of condensation patterns

Treatment of compound **1a** with two equivalents of an Ag$^+$ salt in water yields *cis*-[Pt(H$_2$O)$_2$(NH$_3$)(1-MeC-*N3*)]$^{2+}$ (**2**). The resulting solution is strongly acidic (in D$_2$O, pD 1–2) as a consequence of the acidity of the aqua ligands and formation of *N3,N4*-bridged dinuclear species, which likewise leads to a release of protons from the exocyclic amino group of the 1-MeC ligand. A ^{1}H NMR spectrum recorded after 24 h at RT is given in Figure 3. Typically, 20 % of the diaqua species has been converted under these conditions to a dinuclear [{Pt(D$_2$O)(NH$_3$)(1-MeC$^-$-*N3,N4*)}$_2$]$^{2+}$ species with its chemical shifts at δ = 6.85 (H6), 5.99 (H5) and 3.29 (CH$_3$) ppm (marked with an * in Figure 3). The chemical shifts of the newly formed product are close to values previously seen with head-tail dimers of the composition *cis*-[{Pt(NH$_3$)$_2$(1-MeC$^-$-*N3,N4*)}$_2$]$^{2+}$, and characteristically upfield shifted from those of compounds **1a** and **2** with N3 platinated neutral 1-MeC.[12a]
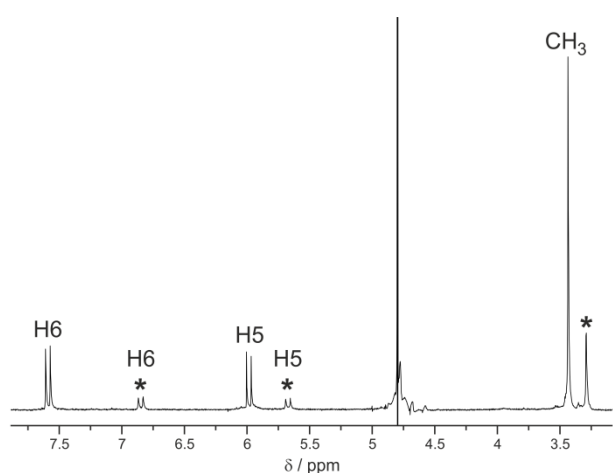
When kept at low pD values (1–2) in D$_2$O, samples of compound **2** undergo isotope exchange of the proton at the C5 position, giving rise to pseudo-triplets of the H6 resonances and a decline of the original H5 doublets (Figures S1 and S2 in the Supporting Information). Readjustment of the pD of the sample to values between 5 and 7 leads mainly to multiple new H5 and H6 doublets around δ = 5.8 and 7.5 ppm, yet also to new weak doublets in the vicinity of the resonances of the initial condensation product marked with asterisks (Figure 4, bottom spectrum, and Figure S3 in the Supporting Information).

As a consequence of the existence of two non-equivalent aqua ligands in compound **2** (Scheme 1), and their expected differences in acidities (see below), there are different possibilities how monomeric compounds **2a** and **2a'** can self-condense to give the head–tail dinuclear complexes **3a**, **3a'**, and **3a''**, respectively. Compound **3a** is achiral, but the two other dimers are chiral, which, if formed, occur as pairs of enantiomers.

Given the closeness in chemical shifts marked with asterisks, there is a good chance that these minor sets are due to any of the other head-tail dimers. From a steric point of view (interference of parallel NH$_3$ and OH$_2$ ligands), the mutual trans arrangement of the bridging 1-methylcytosinato ligands in compounds **3a** and **3a'** may be less favorable than the cis arrangement in compound **3a''**, however.[12b] For an alternative assignment see also below.
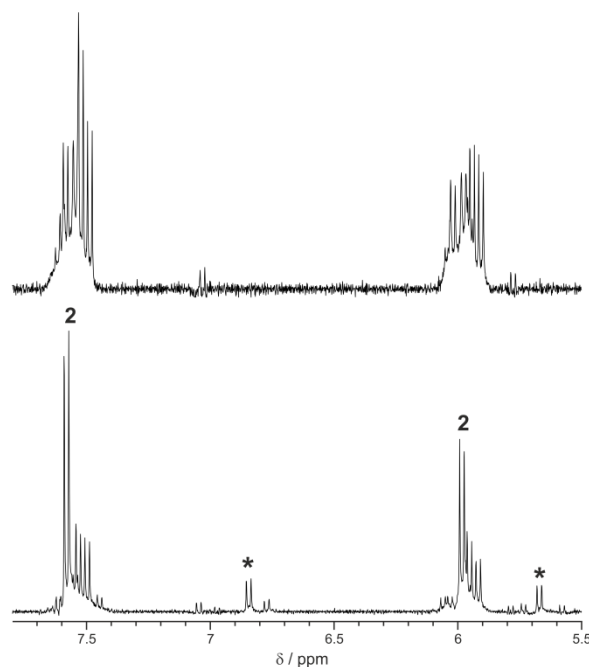

Figure 3. ^{1}H NMR spectrum (200 MHz) of *cis*-[Pt(H$_2$O)$_2$(NH$_3$)(1-MeC-*N3*)]$^{2+}$ (**2**) prepared from compound **1a** and two equivalents of AgNO$_3$ in D$_2$O, RT, 24 h after addition of AgNO$_3$, with c_{Pt} = 0.02 mol/L. Signals with asterisks refer to *N3,N4*-bridged species [{Pt(D$_2$O)(NH$_3$)(1-MeC$^-$-*N3,N4*)}$_2$]$^{2+}$ (see main text). The pD of the solution has dropped to 1.85.

Figure 4. ^{1}H NMR spectra (D$_2$O, 400 MHz) of compound **2** adjusted to different pD values, that is, pD 5.25 (bottom) and pD 6.45 (top). In both cases, the pD value drops within 12 h at RT to approximately 4.1 (5.1). The diaqua species **2** has its 1-MeC resonances unchanged, whereas compounds **2a** and **2b** have undergone condensation reactions to µ-OH species. Signals of the most intense other condensation product with N3,N4 bridge formation (compare Figure 3) are marked by asterisks. Note that there are additional doublets of low intensities close those resonances.
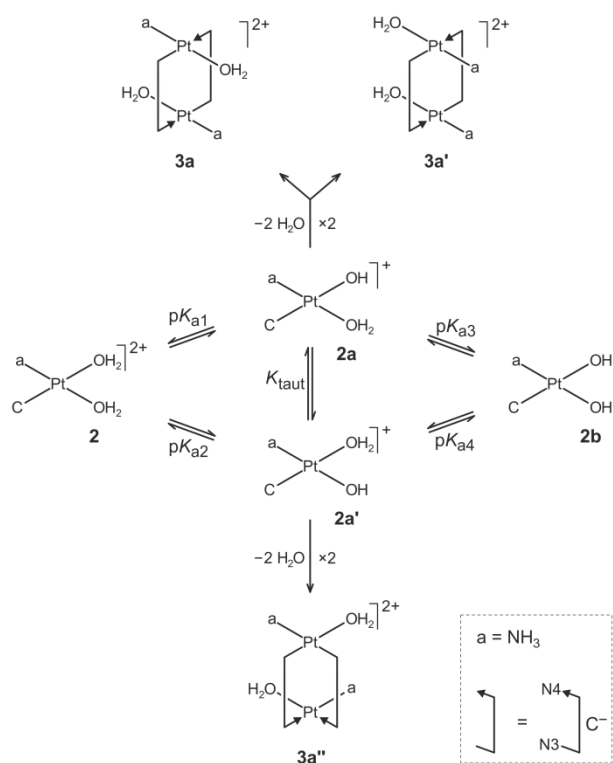
Scheme 1. Acid-base equilibria of compound **2** and feasible dinuclear C⁻ condensation products. Compounds **3a'** and **3a''** are chiral and exist as pairs of enantiomers. A feasible condensation product between compounds **2a** and **2a'** is not shown (see text).

From model building it is possible to construct yet another head–tail dimer, formed between compounds **2a** and **2a'** and assuming that condensation reactions involve again the Pt–OH groups (not shown in Scheme 1). This dinuclear product is likewise chiral, has the bridging cytosinato ligands *cis* at one Pt and *trans* at the other and should give two 1-MeC⁻ sets of equal intensities.

Concerning the acidities of the two non-equivalent aqua ligands of compound **2**, it can be expected that there exist four different pK_a values, which, however, are probably pairwise very similar, hence $pK_{a1} \simeq pK_{a2}$ and $pK_{a3} \simeq pK_{a4}$.

Although the aqua ligand *trans* to 1-MeC can be expected to be slightly more acidic than the one *trans* to the NH₃ ligand,[8b] differences in pK_a values of the two species **2a** and **2a'** cannot be expected to be readily seen in the ¹H NMR spectra, as they represent tautomers.[13] The pD value dependent ¹H NMR spectra of compound **2** in the range 1.8–8.0 reveal the following: The 1-MeC resonances of compound **2** (i.e., species **2a** and **2a'**) display virtually no pD value dependence in the range mentioned. For this reason, pK_a values of the aqua ligands of compound **2** (i.e., species **2a** and **2a'**), expected to be in the order of 5–7,[14] could not be deduced by NMR spectroscopy. The reason for this unexpected behavior is obviously the rapid conversion of mononuclear hydroxo species between the time of pD adjustment and spectra recording. Consistent with this view, resonances of compound **2** only drop in intensities as the pD is raised,

whereas at the same time 1-MeC resonances of the newly formed complexes grow in, at chemical shifts slightly upfield from those of compound **2** (Figure 4).

This finding strongly suggests that Pt coordination in the derivatives occurs still through the N3 atom of the 1-MeC ligand, hence that μ-OH condensation products are formed, similar to the situation with *cis*-[Pt(NH₃)(H₂O)(OH)]⁺.[15] Given the various possible ways of condensation of compounds **2a** and **2a'** (homo- or hetero-condensation, single OH⁻ bridges or cyclic oligomers, compare compounds **4a–4e** in Scheme 2), it is not possible to individually assign the various signals seen in the ¹H NMR spectra. Analogous μ-OH species seem not to be observed with 2- and 3-picoline complexes *cis*-[Pt(H₂O)₂(NH₃)(pic)]²⁺,[6] at least not at a fourfold lower concentration (5 mM). In contrast, compound **2** undergoes μ-OH condensation, even at a concentration of 5 mM, with the corresponding resonances seen quickly after pD adjustment.
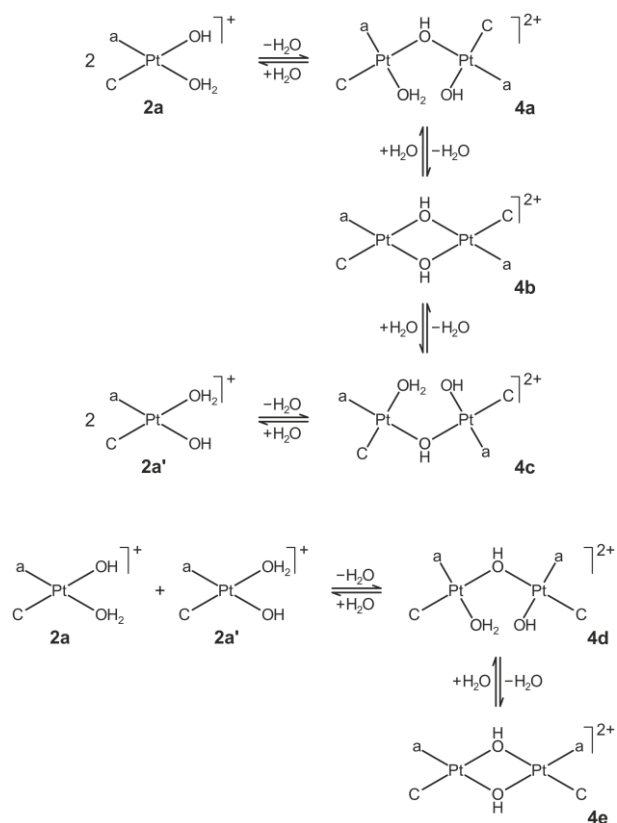
Scheme 2. Feasible condensation reactions of compounds **2a**, **2a'** leading to the dinuclear μ-OH species **4a–4e**. In analogy to *cis*-[Pta₂(H₂O)(OH)]⁺ also tri-and tetranuclear μ-OH species are feasible.

There is a third possibility by which condensation reactions can occur involving a ligand deprotonation process, namely μ-NH₂ bridge formation. Although less unexpected for Pt complexes with oxidation states +III and +IV,[16] μ-NH₂ complexes are also known for diplatinum(II) species isolated from aqueous solution,[17] including 1-MeC-containing compounds.[18,19]

All three mentioned condensation reactions leading to μ-OH, μ-NH₂, or μ-1-MeC⁻ species require

deprotonation of ligands (H₂O, NH₃, or 1-MeC, respectively). There exists, however, also the possibility that condensation does not involve loss of protons, namely if bridge formation is through the N3 and O2 atoms of the neutral 1-MeC ligand, with only water ligands being replaced. Indeed, X-ray crystal structures are available for such N3,O2 binding patterns in complexes of Ag^+,[20a] Zn^{2+},[20b] and heteronuclear complexes containing Pt^{2+} at the N3 position and a second transition metal ion at the O2 position.[20c,20d] From a structural point of view, dinuclear complexes should be analogous to compounds **3a**, **3a'**, and **3a''** (with the N4 atom being replaced by the O2 atom), but there is a question whether the O2(1-MeC) bond to Pt is inert or labile in aqueous solution. We tend to believe that the latter is the case and, therefore, do not further discuss the option of N3,O2 bridge formation here. In any case, the experimental observations of a drop in the pH value following preparation of the diaqua complex **2** is inconsistent with N3,O2-bridge formation being a dominant reaction.

Finally, there may be an additional complication in the behavior of compound **2** (i.e., species **2a** and **2a'**), namely the possibility of Pt^{II} migration from the N3 position to the exocyclic N4 position. Resonances of the Pt(1-MeC-*N4*) species can be spread over a considerable shift range,[21] and some of the very weak H5,H6 doublets seen in the bottom spectrum of Figure 4 in fact may be due to such compounds.[22] Unfortunately the quality of signal-to-noise ratio of ¹H NMR spectra recorded at higher pD values (i.e., pD 7–8) is decreasing, and these minor resonances are no longer observable.

Partial oxidation

The disappearance of resonances due to *N3,N4*-bridged 1-MeC⁻ species in the ¹H-NMR spectra may be a consequence of the formation of paramagnetic, partially oxidized mixed-valence Pt compounds. Samples of aqueous solutions of compound **2** become greenish within 20 h (max. absorption at λ = 607 nm), with a continuous increase in color and intensity and a shift of the major absorption towards higher wavenumbers (λ = 634 nm). At the same time a second absorption near λ = 442 nm grows (Figure S4 in the Supporting Information). Concentration dependent UV/Vis spectra reveal an essentially linear relationship with the two bands in the concentration range 0.2–2.0 µmol/mL of Pt. Extinction coefficients could not be determined, as the concentration of the colored species is unknown. We contribute at least the absorption above λ = 600 nm to an intervalence charge-transfer (CT) band, similar to the situation with other "platinum pyrimidine blues".[23] The mixed valence of species in aged samples of compound **2** is qualitatively confirmed by EPR spectroscopy (Figure S5 in the Supporting Information) of frozen aqueous solutions. The EPR spectra are similar to previously reported ones, suggesting axially interacting Pt^{II} and Pt^{III} centers.[24] As compared to a published spectrum of a

Pt^{II}/Pt^{III} complex of cis-(NH₃)₂Pt and cytidine,[24b] the spectral lines are considerably broader in our case, possibly suggesting a higher degree of Pt oxidation and/or the presence of different, albeit structurally similar paramagnetic species.

Figure 5 shows ESI mass spectra of cis-[Pt(H₂O)₂(NH₃)(1-MeC-*N3*)](NO₃)₂ recorded after 1d and after 3d (c_{Pt} = 0.02 M). Different target masses were applied while recording the spectra, causing changes in relative intensities of peaks and hence in the overall appearance of the spectra. Nevertheless, a detailed look reveals the appearance of new signals with time and in addition *time dependent* changes of individual signals.

Mass spectra of compound 2 and its condensation and oxidation products

As pointed out above, the diaqua species cis-[Pt(H₂O)₂(NH₃)(1-MeC-*N3*)]²⁺ (**2**) undergoes preferentially two types of condensation reactions in water, involving at low pH preferably the 1-MeC ligands, and at weakly acidic to neutral pH the OH₂/OH ligands. In the first case, 1-MeC⁻-*N3,N4* bridged species are subject to facile oxidation in the presence of air (see above) leading to deeply colored mixed-valence Pt compounds initially. In the following we describe results obtained from ESI mass spectra of compound **2** at different time intervals. We were hoping to get a deeper insight into the species present in solution, even though we were aware that no real complementarity exists between this method and ¹H NMR spectroscopy,[25] in that essentially only +1 cations are detected under the conditions of ESI MS, and that the distribution of species present in solution is not reflected by relative intensities of the peaks in the mass spectra. Finally, the uncertainty concerning fragmentation or association processes in the gas phase poses further questions.

Figure 5 shows ESI mass spectra of cis-[Pt(H₂O)₂(NH₃)(1-MeC-*N3*)](NO₃)₂ recorded after one day and after three days (c_{Pt} = 0.02 M). Different target masses were applied while recording the spectra, causing changes in relative intensities of the peaks and hence in the overall appearance of the spectra. Nevertheless, a detailed look reveals the appearance of new signals with time and in addition time-dependent changes of individual signals.

Aged samples of compound **2** (see, e.g., Figure 5, bottom) reveal characteristic "families" of signals, centered around m/z = 1650, 1350, 1024, and 706. Clearly these "families" represent species of different stoichiometries (Pt/1-MeC/1-MeC⁻) as outlined below. Within a "family" signals differ typically by Δm = 17 or 18, suggesting differences in NH₃ and H₂O contents. Each signal itself reveals characteristic isotopic patterns. With very few exceptions, the spacing between these fine structure lines is one nominal mass unit, indicating +1 charges for most ions.
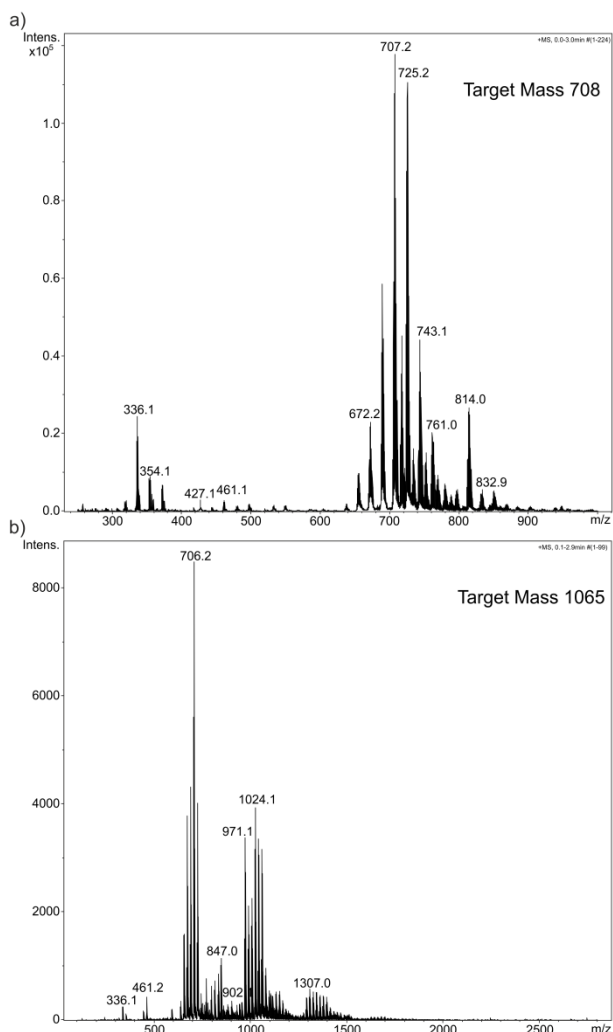
Figure 5. ESI mass spectra of aqueous solution of compound **2** after a) one day (target mass = 708) and b) three days (target mass = 1065). The complex concentration was 0.02 M. Note: To improve the ion storage in different mass regions, different target mass parameters were applied.

There is a general problem of assigning the individual signal groups to particular structures of the Pt complexes for the following reasons: 1) Complexes may exist in different tautomeric forms or even in equilibria of tautomers. For example, a dinuclear complex could have a μ-OH^- bridge and a terminal NH_3 ligand or alternatively a μ-NH_2^- bridge and a terminal H_2O ligand. The sum of the two charges is identical in both cases. Similarly, the combinations of OH^- and 1-MeC or of H_2O and 1-MeC$^-$ are identical. 2) The almost identical masses of NH_3 and OH^- permit a differentiation in high resolution mass spectrometry only. This feature can cause an ambiguity regarding relevant Pt oxidation states as well, in that combinations of Pt^{II}–NH_3 and Pt^{III}–OH^- would be difficult to differentiate. From a coordination chemistry point of view, the conversion of a Pt^{II}–NH_3 moiety to a Pt^{III}–OH^- would definitely be reasonable, considering the fact that any Pt^{III}–NH_3 bond of the d^7 metal ion can be expected to be much more labile than of the d^8 metal ion Pt^{II}. Consequently, a reaction of type $[Pt^{III}$–$NH_3]^{n+} + H_2O \rightarrow [Pt^{III}$–$OH]^{(n-1)+} + NH_4^+$ is a realistic

option, even in solution.[12,26] 3) When working with the nitrate salt of compound **2**, there is the additional problem of differentiating the almost identical masses of 1-MeC$^-$ (m = 124) and two NO_3^- anions (m = 2 × 62 = 124). Of course, this ambiguity can be circumvented by use of a different counterion, for example ClO_4^- or BF_4^- instead of NO_3^-.

A typical mass spectrum of *cis*-[Pt(H_2O)$_2$(NH_3)(1-MeC-*N3*)](NO_3)$_2$, 24 h after mixing *cis*-[PtCl$_2$(NH_3)(1-MeC-*N3*)] with AgNO$_3$ in water (c_{Pt} = 0.02 M; pH = 1.9 after 24 h; the color of solution is light green) reveals signals due to mononuclear complexes centered at *m/z* = 372, 354, and 336. They correspond to [Pt(OH^-)(H_2O)(NH_3)(1-MeC-*N3*)]$^+$ as well as species containing chelating 1-MeC (N3,O2)[27] or chelating 1-MeC$^-$ (N3,N4) ligands[28] (Scheme S1 in the Supporting Information).

The cluster of signals between *m/z* = 761 and 655, which has its most intense peaks at *m/z* = 707 and 725, corresponds to a group of dinuclear Pt complexes.

There is a large variety of possible structures for this "family", as outlined in Schemes 3 and 4, depending on the bridging ligands, 1-MeC$^-$ or OH^-. Figure 6 gives an
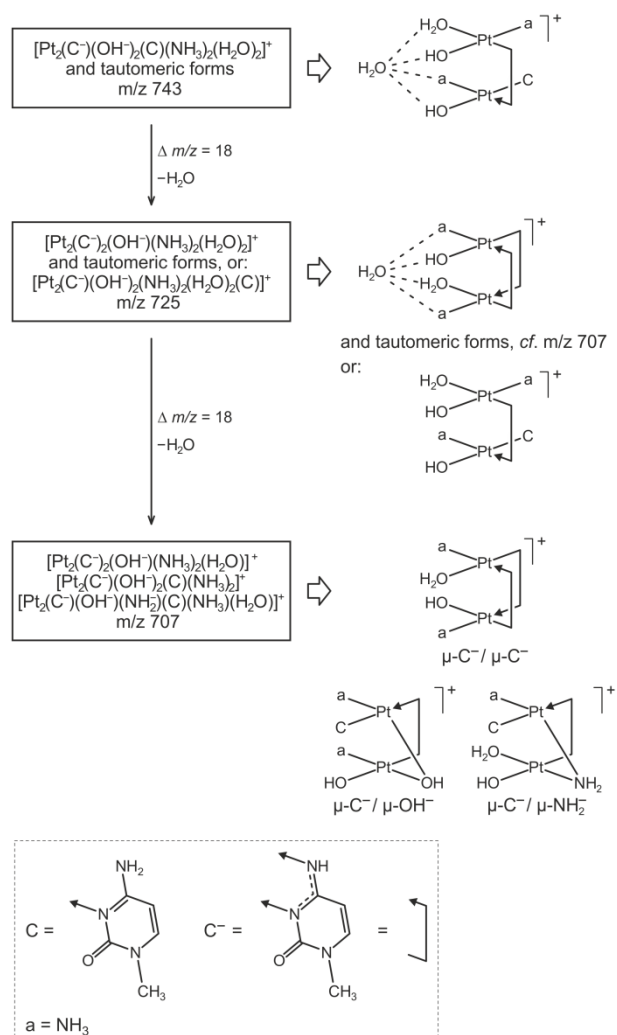
Scheme 3. Suggested structures for complexes of *m/z* = 743 to 707 formed by loss of H_2O either through condensation reactions or through the loss of originally bonded aqua ligands.

–6–

enlargement of the experimental signal centered at $m/z = 707$ and a simulated spectrum for $[Pt_2(1\text{-}MeC^-\text{-}N3,N4)_2(OH^-)(NH_3)_2(H_2O)]^+$. Despite the generally good agreement between the two spectra, there is the question (see intensities of the $m/z = 704$ signal) whether the experimental spectrum represents in fact the superposition of $m/z = 707$ and a small fraction of a species centered at $m/z = 706$, hence of $[Pt^{II}Pt^{III}(1\text{-}MeC^-\text{-}N3,N4)_2(NH_3)_2(OH)_2]^+$ (see also the section on the mass spectrometric results of compound **7**).
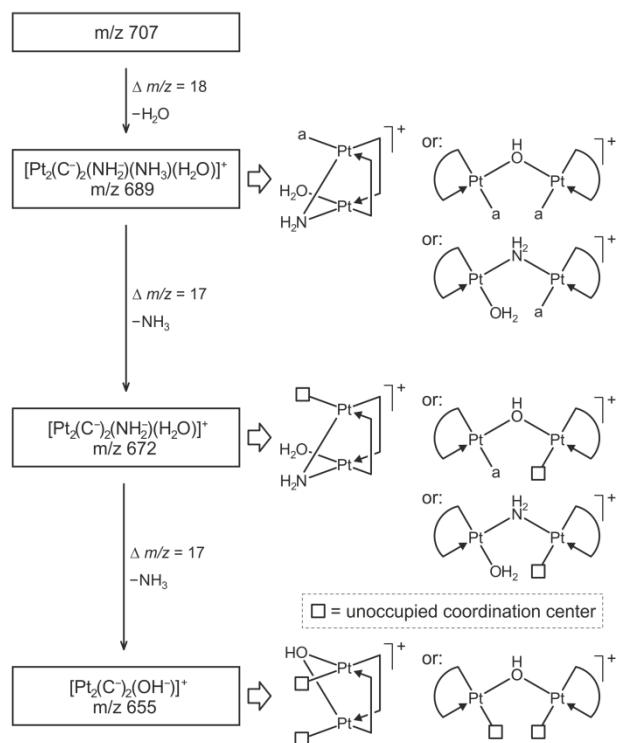
Scheme 4. Suggested structures for complexes of $m/z = 707$ to 655 formed by the loss of H_2O or NH_3, with different bridging modes of the Pt^{II} centers.
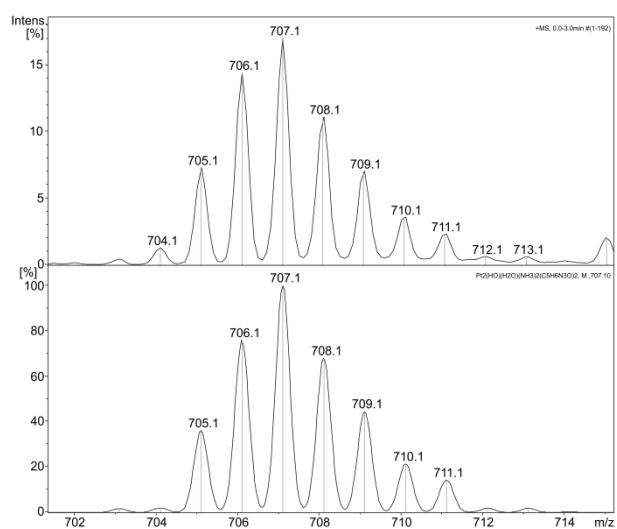

Figure 6. Fine structure of the $m/z = 707$ ESI-MS peak after a reaction time of one day (top) and simulated spectrum for $[Pt_2(1\text{-}MeC^-\text{-}N3,N4)_2(OH^-)(NH_3)_2(H_2O)]^+$ (bottom). The signal at $m/z = 704$ suggests a superposition with a minor species centered at $m/z = 706$ which is consistent with observations in aged solutions.

The "family" just discussed is partially overlapping with another one with maxima at $m/z = 770$, 752, 734, and 717. These species can be assigned to diplatinum(II) complexes containing coordinated and/or electrostatically bonded NO_3^- ions (Scheme S2, Supporting Information). This interpretation seems reasonable considering the fact that this set of signals is not observed when the diaqua species **2** is applied as its BF_4^- salt.

Ageing of the diaqua species **2** (3 d, RT) leads to new signals, the characteristics of which are as follows: Firstly, tri- and tetranuclear Pt complexes form, centered at around $m/z = 1024$ and 1350. There is even a group of peaks centered at $m/z = 1650$, which, however, is too low in intensity to be discussed here. It would, logically, correspond to a pentanuclear Pt species. Secondly, the signals due to dinuclear complexes undergo shifts to lower m/z values with time. Regarding the second case, the signal with a maximum at $m/z = 707$ shifts to have its maximum at $m/z = 706$ after three days. This feature is consistent with a mixture of two singly charged cations being present in the sample, which differ by a mass of one (Figure 7).

A similar shift occurs for the peaks at $m/z = 689$ (shift to 688) and $m/z = 672$ (shift of maximum to $m/z = 671$). The most logical interpretation of this loss of one mass unit and simultaneous maintenance of charge is a substitution of a Pt^{II}–H_2O entity by a Pt^{III}–OH unit. In fact, an increase in Pt oxidation state is expected to cause a drop in pK_a of any coordinated ligand, including water. Alternatively, this process can be seen as a proton-coupled electron transfer reaction, namely formally: $2\ [X\text{–}Pt^{II}\text{–}OH_2]^+ + \frac{1}{2}\ O_2 \rightarrow 2\ [X\text{–}Pt^{III}\text{–}OH]^+ + H_2O$ (with X = ligand with negative charge; other ligands omitted). As far as dinuclear species are concerned, this implies the formation of mixed valence Pt^{II}/Pt^{III} species. Possible structures are formulated in Scheme 5.
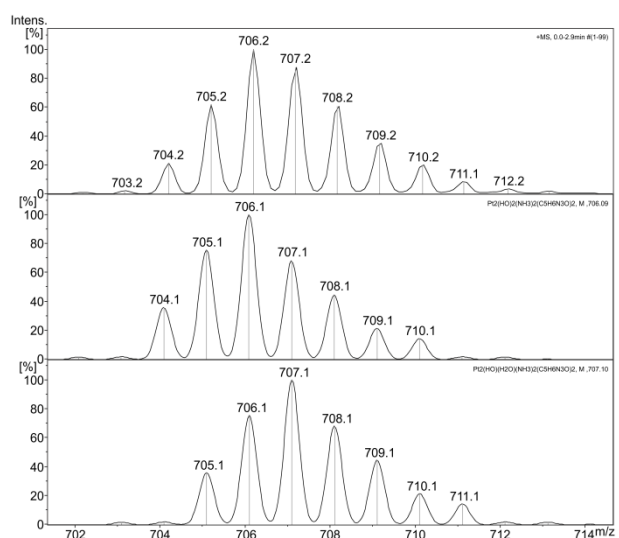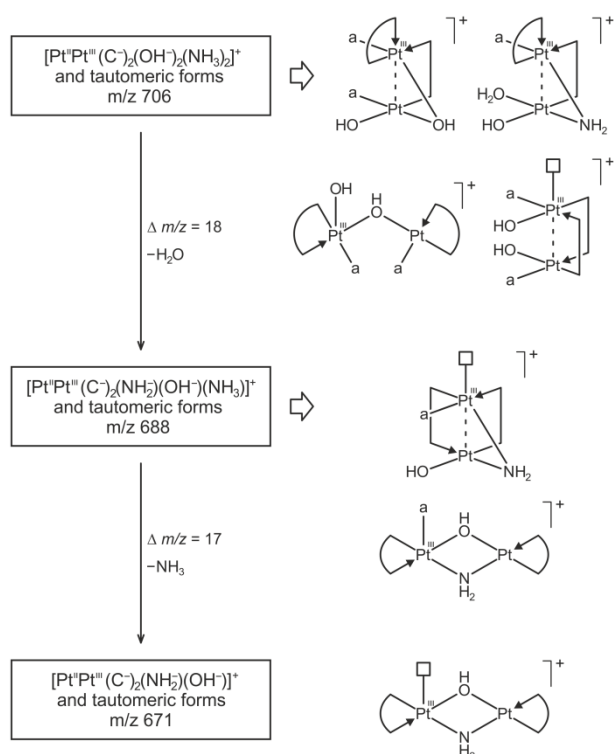

Figure 7. ESI mass spectra of compound **2**: Fine structure for the signal at $m/z = 706$ after 3 d (top) with simulated spectra for $[Pt_2(1\text{-}MeC^-\text{-}N3,N4)_2(OH^-)(NH_3)_2(H_2O)]^+$ ($m/z = 706$; middle) and $[Pt_2(1\text{-}MeC^-\text{-}N3,N4)_2(OH^-)_2(NH_3)_2]^+$ ($m/z = 707$).(below).

Scheme 5. Proposed structures for mixed valence complexes of m/z = 706 to 671 formed by loss of H_2O or NH_3. Alternative tautomeric forms are not included.

Yet another "family" of MS peaks, occurring between m/z = 832 and 762, is identified, which corresponds to complexes of a Pt_2L_3 (L = 1-MeC or 1-MeC$^-$) stoichiometry. The number of possible structures and combinations of Pt oxidation states becomes increasingly larger for these peaks (Scheme S3 in the Supporting Information).

Trinuclear Pt complexes of a stoichiometry of Pt_3L_3 give rise to a cluster of intense peaks in the range m/z 1000–1100. The number of feasible structures, either linear or cyclic, increases tremendously, as does the combination of possible Pt oxidation states (Scheme S4 in the Supporting Information). It suffices to state that there is precedence for the existence of cyclic, 1-MeC$^-$ bridged trimeric complexes of analogous Pd$^{II[29]}$ and Pt^{II} complexes,[30] and of mixed OH$^-$, 1-MeC$^-$ bridged species,[31] among others. Consequently, it can be concluded that the proposals made are chemically realistic. Likewise, formation of such species (cyclic or linear) from the initial monomer [Pt(OH)(H$_2$O)(NH$_3$)(1-MeC-*N3*)]$^+$ is readily rationalized (Scheme S5 in the Supporting Information). Again, by applying the replacement of Pt^{II}–H$_2$O by Pt^{III}–OH$^-$ partially oxidized Pt complexes can be postulated, as shown in Figure 8 for species for the signal at m/z = 1077.

As a final group of signals, we shall examine those related to tetranuclear Pt_4L_4 complexes of aged samples. This family of peaks occurs above m/z = 1300. Again, there are numerous feasible structures, which could account for the masses experimentally observed, which include cyclic as well as open-chain structures
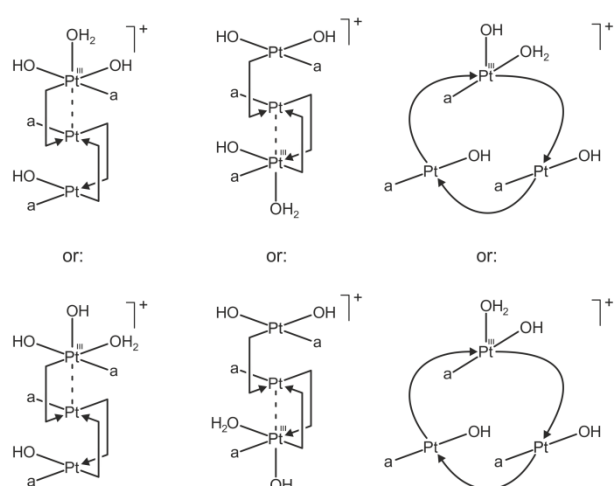

Figure 8. Different feasible structures for mixed-valence complexes with m/z = 1077, either in linear or cyclic arrangements.

with simultaneous 1-MeC$^-$, OH$^-$, and/or NH$_2^-$ bridge formation. Thus far, we have not discussed the feature of mixed 1-MeC$^-$, OH$^-$, NH$_2^-$ bridging in detail yet, but it must be pointed out that there is structural evidence for the existence of curved Pt_2M_2 (M = Pd[18] or Pt[19]) skeletons with all of the three mentioned bridges present in a single complex. Feasible structures of [Pt^{II}]$_4$ species displaying this feature are shown in Scheme 6. It should be noted that the experimentally observed mass spectra reveal the above-discussed shifts to lower masses, hence the existence of partially oxidized complexes. Figure 9 compares the MS peaks centered at around m/z = 1395 and a simulated spectrum of a tetranuclear complex of the composition [Pt$_4$(1-MeC$^-$)$_2$(1-MeC)$_2$(NH$_3$)$_2$(NH$_2^-$)(OH$^-$)$_2$]$^+$ (m/z = 1395.18). The experiment clearly reveals a superimposition with one or more species of lower mass, for example, m/z = 1394 and/or 1393.
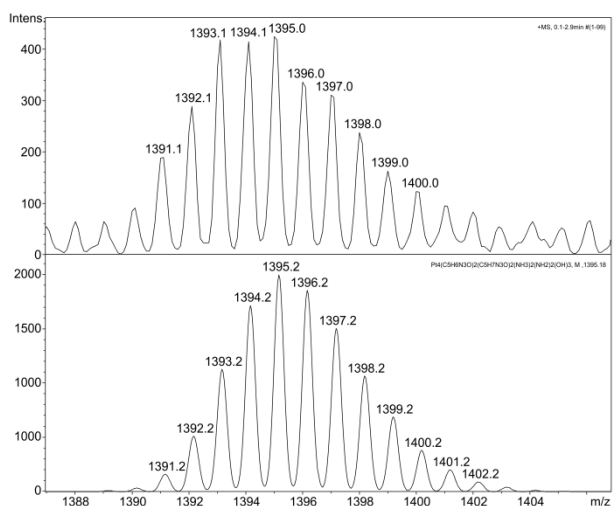
Figure 9. ESI-MS peak m/z = 1395 (top) with simulation for [Pt$_4$(1-MeC$^-$-*N3,N4*)$_2$(1-MeC-*N3*)$_2$(OH$^-$)$_3$(NH$_3$)$_2$(NH$_2^-$)$_2$]$^+$ (bottom). The Pt concentration was 0.02 M, target mass was 1065. The observed peaks indicate superimposition with species of lower m/z such as 1394 and/or 1393.
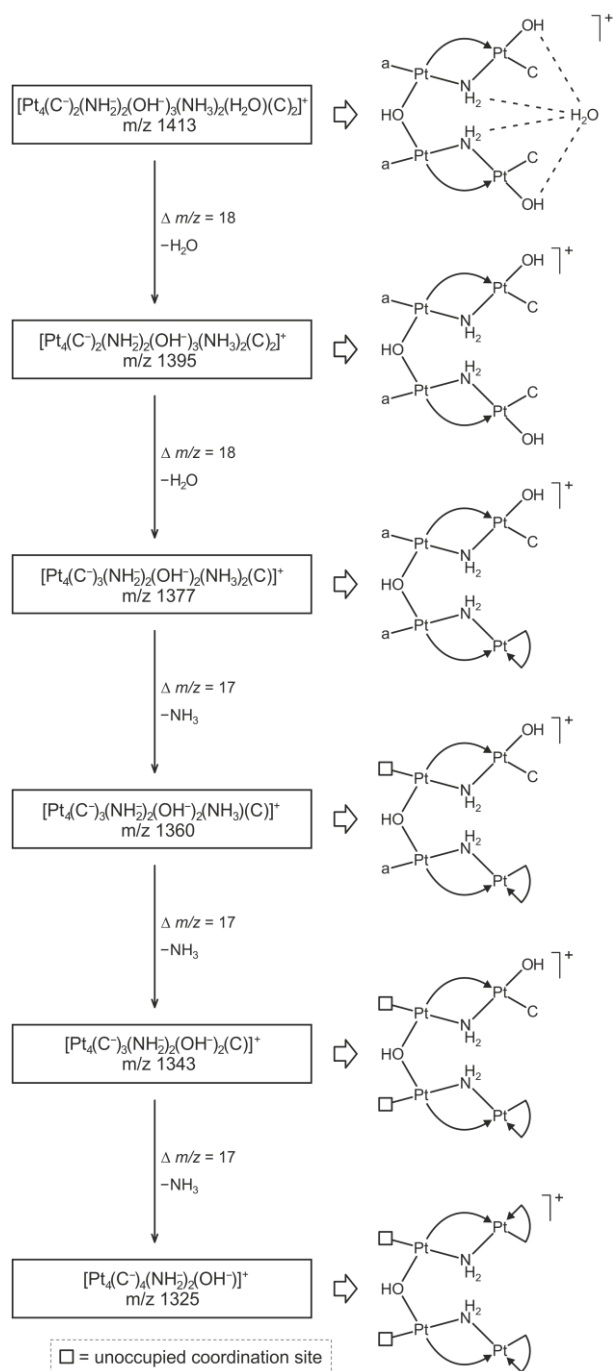
Scheme 6. Proposed decomposition processes based on a tetranuclear species with m/z = 1413 involving loss of H_2O and NH_3 respectively, leading eventually to a fragment with m/z = 1325.

Models of potential DNA adducts of 1a with guanine targets

Assuming that the activity of compound **1a** in tumor models (see below) is a consequence of DNA binding, and assuming further that the guanine-N7 sites are preferred binding sites of compound **1a** as in the case of cisplatin, a reaction scheme is possible which leads to three products (Scheme 7), that is, SP-4-4-[PtCl(NH$_3$)(1-MeC-*N3*)(G-*N7*)]⁺, SP-4-2-[PtCl(NH$_3$)(1-MeC-*N3*)(G-*N7*)]⁺ and cis-[Pt(NH$_3$)(1-MeC-*N3*)(G-*N7*)$_2$]²⁺ (with SP = square-planar, and G = guanine base in double-stranded (ds)-DNA).[32] In principle, all three products can occur as multiple stereoisomers if rotation around

the Pt–N(nucleobase) bonds is hindered and consequently different mutual orientations of the two or three heterocyclic rings can exist.[33]
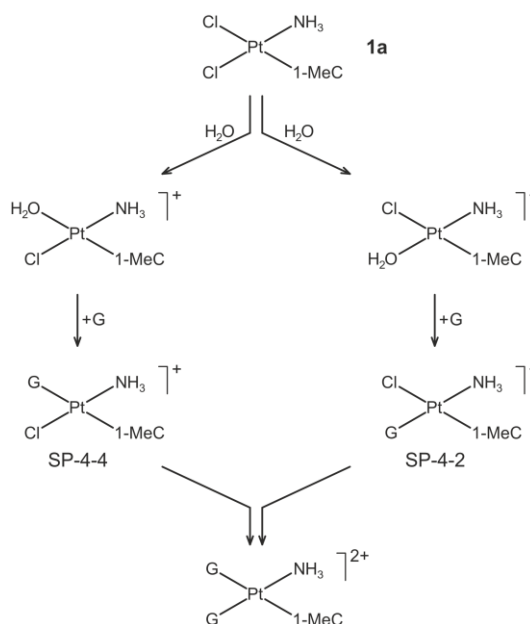
Scheme 7. Possible pathways for the formation of cis-[Pt(NH$_3$)(1-MeC-*N3*)(G-*N7*)$_2$]²⁺ (with G = guanine base in ds-DNA) from compound **1a** through SP-4-4-[PtCl(NH$_3$)(1-MeC-*N3*)(G-*N7*)]⁺ and through SP-4-2-[PtCl(NH$_3$)(1-MeC-*N3*)(G-*N7*)]⁺.

The scheme reveals that compound **1a** not only can behave like cisplatin, hence can form G,G intrastrand adducts (end product), but also monodentate DNA adducts (SP-4-4 and SP-4-2) are feasible, in which the 1-MeC ligand of compound **1a** is located in the major groove of DNA, similar to the situation observed for binding of monofunctional cis-[Pt(NH$_3$)$_2$(py)Cl]⁺ (py = differently substituted pyridines) to ds-DNA.[7] Clearly, the stereochemical situation is different for the SP-4-4 and SP-4-2 adducts, but any polymerase activity might be seriously affected by either adduct. With the end product cis-[Pt(NH$_3$)(1-MeC-*N3*)(G-*N7*)$_2$]²⁺ the well-established kinking of DNA[34] is to be expected, hence one might speculate on a synergy of two effects regarding the proper function of DNA. For picoplatin, Sadler et. al. have prepared and structurally characterized a model of the corresponding end product cis-[Pt(NH$_3$)(picoline)(G-*N7*)$_2$]²⁺.[35] In the solid state, the two guanine bases, both bonded to Pt via N7 sites, adopt a head-tail orientation, with their H8 resonances practically indistinguishable in neutral to weakly acidic aqueous medium. In any case, only a preferred stereoisomer, yet not a complicated mixture, is present in solution.

Starting out from compound **1a**, we decided to learn more about the sequence of steps leading to cis-[Pt(NH$_3$)(1-MeC-*N3*)(G-*N7*)$_2$]²⁺ by reacting the dichloride complex **1a** with 9-EtGH (9-ethylguanine) as a model for a guanine base in ds-DNA. Figure 10 gives representative ¹H NMR spectra of mixtures of compound **1a** with 9-EtGH (1:1 and 1:2) after different reaction times in D$_2$O, pD ≈ 6, at room temperature.
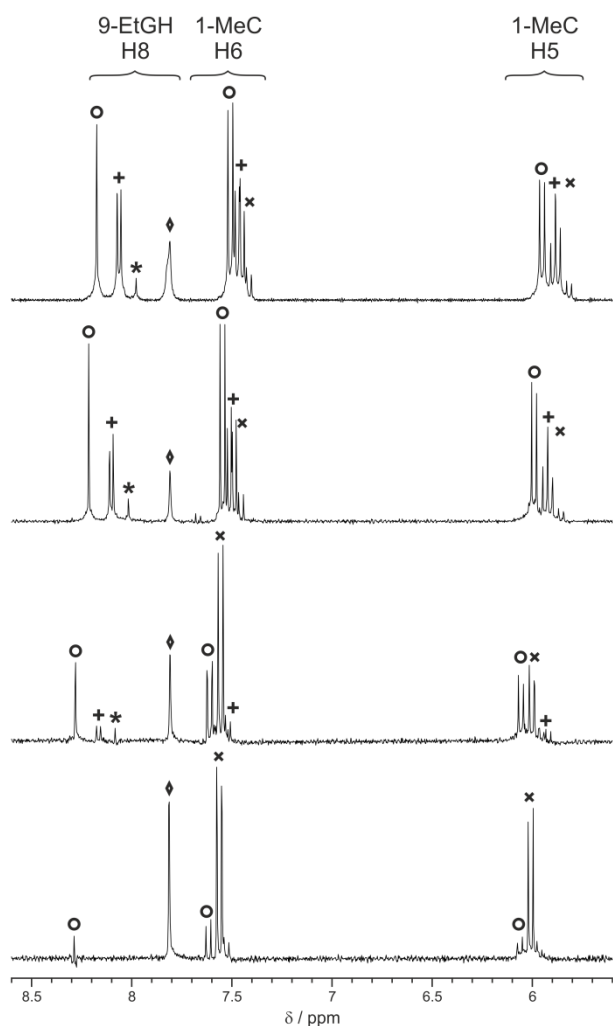
Figure 10. ^{1}H NMR spectra (300 MHz) of the reaction of compound **1a** with one equivalent of 9-EtGH at RT in D_2O after 24 h, 48 h, 3 d, 8d (bottom to second from top), and two equivalents 9-EtGH after 3 d (top, pD 6). Detail of the shift range of heteroaromatic protons. (o = SP-4-4-[PtCl(NH$_3$)(1-MeC-*N3*)(9-EtGH-*N7*)]$^+$, * = SP-4-2-[PtCl(NH$_3$)(1-MeC-*N3*)(9-EtGH-*N7*)]$^+$, x = *cis*-[PtCl$_2$(NH$_3$)(1-MeC-*N3*)] (**1a**) + = *cis*-[Pt(NH$_3$)(1-MeC-*N3*)(9-EtGH-*N7*)$_2$]$^{2+}$, ◊ = free 9-EtGH).

The first product to be detected in the ^{1}H NMR spectrum is assigned to SP-4-4-[PtCl(NH$_3$)(1-MeC-*N3*)(9-EtGH-*N7*)]$^+$, hence to a species in which 1-MeC-*N3* and 9-EtGH-*N7* are oriented trans to each other. The arguments are as follows: First, the Cl ligand trans to 1-MeC in compound **1a** is expected to hydrolyze faster than the Cl ligand cis to the 1-MeC ligand, as steric bulk of the two exocyclic groups of 1-MeC (O2 and N4H$_2$) in the trigonal-bipyramidal (tbp) transition state is expected to slow down substitution kinetics of the chlorido ligand cis to the 1-MeC ligand by water. Second, the chemical shift of the H8 resonance of the 9-EtGH ligand of the first product formed (δ = 8.37 ppm) compares favorably well with that in *trans*-[Pt(NH$_3$)$_2$(1-MeC-*N3*)(9-EtGH-*N7*)]$^{2+,}$[36] whereas in the corresponding cis isomer, this resonance occurs at higher field, δ = 8.18 ppm[37] as a consequence of the π-stacking effect of the 1-MeC ligand.

At a later stage, three more H8 resonances of coordinated 9-EtGH ligands are observed: A weak singlet at δ = 8.17 ppm, assigned to SP-4-2-

[PtCl(NH$_3$)(1-MeC-*N3*)(9-EtGH-*N7*)]$^+$ and consistent with a slower hydrolysis rate of the Cl ligand cis to the 1-MeC ligand, as well as two singlets of equal intensities at δ = 8.28 and 8.29 ppm. The latter resonances are assigned to the two non-equivalent 9-EtGH ligands in the end product *cis*-[Pt(NH$_3$)(1-MeC-*N3*)(9-EtGH-*N7*)$_2$]$^{2+}$.

When compound **1a** and 9-EtGH are reacted in a 1:2 ratio under otherwise similar conditions of pH and temperature, the bis(9-ethylguanine) product is the dominant species after sixteen days. In the absence of X-ray structural evidence no firm conclusions regarding the relative orientations of 9-EtGH and 1-MeC ligands in *cis*-[Pt(NH$_3$)(1-MeC-*N3*)(9-EtGH-*N7*)$_2$]$^{2+}$ are possible. Given the sharpness of the guanine resonances of all the products and considering the steric congestion around the central metal caused by the three coordinated nucleobases, we tend to favor a situation without fast nucleobase rotation, however. An isomer of the end product, *trans*-[Pt(NH$_3$)(1-MeC-*N3*)(9-EtGH-*N7*)$_2$]$^{2+}$, obtained by reaction of *trans*-[Pt(H$_2$O)$_2$(NH$_3$)(1-MeC-*N3*)]$^{2+}$ with 9-EtGH, has earlier been reported by us.[38]

trans-[PtX$_2$(NH$_3$)(1-MeC-N3)] [X = I (5a), Br (5b)]

We have previously described the synthesis of the trans isomer of compound **1a**, *trans*-[PtCl$_2$(NH$_3$)(1-MeC-*N3*)], and its X-ray crystal structure,[39] as well as the synthesis of *trans*-[PtI$_2$(NH$_3$)(1-MeC-*N3*)] (**5**).[9] We have now obtained **5** in a slightly modified way (compare to Experimental Section) and furthermore a DMF adduct of 5, trans-[PtI2(NH3)(1-MeC-N3)]·DMF (**5a**), the crystal structure of which was determined. Starting from **5**, the bromide analogue *trans*-[PtBr$_2$(NH$_3$)(1-MeC-*N3*)] (**5b**) was also prepared and isolated as single crystals suitable for X-ray crystallography. Like its chlorido analogue, compound **5** has been proven a useful precursor for the synthesis of tris(nucleobase) complexes derived from an original *cis*-(NH$_3$)$_2$Pt^{II} entity,[11] for square-planar Pt complexes with up to four different ligands,[40] as well as for 1-MeC$^-$ bridged diplatinum(III) species.[9]

Figure 11 shows the structures of compounds **5a** and **5b**. As expected, the 1-MeC planes form large dihedral angles in **5a** (82.04(15)°) and **5b** (74.9(2)°), and the iodido ligands are somewhat bent away from the 1-MeC plane, resulting in a smaller I–Pt–I angle than the ideal 180°, namely 173.972(18)°. For compound **5b**, this effect is less pronounced (178.88(4)°). Otherwise there are no unexpected structural features to be seen (Table S2 in the Supporting Information).
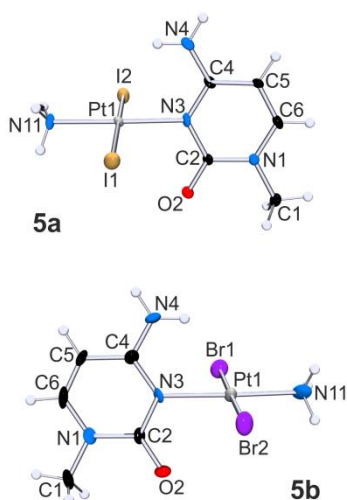
Figure 11. Views of complexes **5a** and **5b** with atom numbering schemes. Ellipsoids are drawn at the 30% probability level.

Solution behavior of compound 5a and of its diaqua species 6

Compound **5** and **5a** are poorly soluble in water. Compound **5** and **5a** are well soluble in DMF, however (Figure S6 in the Supporting Information). Removal of the iodido ligands of either compound by using AgNO₃ in D₂O yields *trans*-[Pt(D₂O)₂(NH₃)(1-MeC-*N3*)]²⁺ (**6**), which is subject to rapid condensation, accompanied by a drop in the pD value, partial oxidation of Pt and development of an intensive purple color (λ_{max} = 516 and 630 nm). The EPR signal of a frozen solution is characteristic of a mixed-valence species as previously reported.[9] For MS studies with compound **6** (non-deuterated), see below. According to ¹H NMR spectroscopy and the X-ray structure of a diplatinum(III) derivative,[9] the primary condensation product at low pH is the head–tail dinuclear complex **7** (Scheme 8). As the two aqua/hydroxido ligands in compound **7** are equivalent, condensation reactions between OH groups and N4H₂ sites of the 1-MeC ligand lead to a single product **7**, unlike in the case of compounds **2a** and **2a'**. Like species **3a''**, compound **7** is also chiral and is formed as a pair of enantiomers.
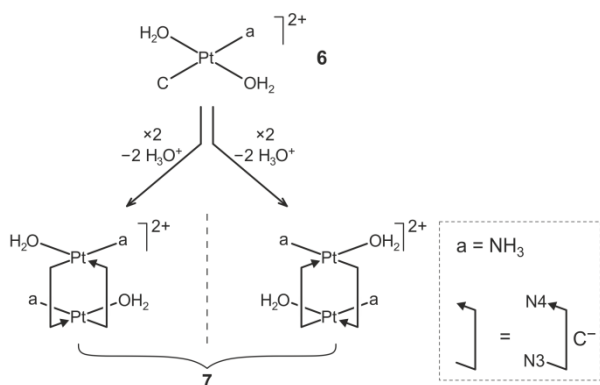
Scheme 8. Formation of the *ht*-dimer **7**. It is formed as a pair of enantiomers.

As the pD is raised during the ageing process new resonances of possibly open μ-OH bridged species can be observed in the corresponding ¹H NMR spectra, similar to those shown for the *cis*-isomer **2**.

Isomeric head-tail dimers 3a'' and 7. Comparison with compound 8

Compounds **3a''** and **7** are isomers, which differ in the positioning of the NH₃ and H₂O ligands. These are inverted in the two compounds: In compound **7** the H₂O ligand is trans to the N4 position of the 1-MeC⁻ ligand. A comparison of the ¹H NMR chemical shifts of the 1-MeC⁻ ligands in compounds **3a''**, **7**, and that of *ht-cis*-[{Pt(NH₃)₂(1-MeC-*N3,N4*)}₂]²⁺ (**8**)[12a] strongly suggests closely similar structures for all three compounds (Table 1). As head–tail dinuclear structures have been established (**8**) or made highly likely (**7**), we propose an analogous head-tail dinuclear composition for the main condensation product of compound **2**, hence for **3a''** (compare Scheme 1). The minor difference in the H5 chemical shift between compounds **3a''** and **8** appears to be a consequence of the different trans influences of the H₂O (in compound **3a''**) and NH₃ ligands (in compounds **7** and **8**).

**Table 1.** ¹H NMR chemical shifts of dinuclear complexes **3a''**, **7**, and **8**.

	H6	H5	CH₃
3a''	6.85 d; 7.6 Hz	5.67 d	3.29 s
7	6.85 d; 7.3 Hz	5.76 d	3.30 s
8	6.88 d; 7.5 Hz	5.74 d	3.29 s

Of the three +2 cations, compound **7** is most sensitive toward oxidation in air, followed by compound **3a''** and finally compound **8**. Although diplatinum(III) complexes of compound **8** have been prepared in several cases by treatment with strong oxidants,[41,42] compound **8** retains its faint yellow color for a long time in aqueous solutions exposed to air. In contrast, aqueous solutions of the diaqua species **7** become quickly purple (few hours), and aqueous solutions of the diaqua species of compound **2** develop a green and later a brownish color more slowly (>24 h) under comparable conditions of pH and concentration. It is obvious that the presence of the good leaving group H₂O in compounds **3a'** and **7** could facilitate further condensation reactions beyond the dinuclear level, in principle, with involvement of the O2 sites of the 1-MeC⁻ bridges. Pt oxidation may be eased in this case. It is interesting to note that *cis*-[PtCl(NH₃)₂(1-MeC-*N3*)]⁺, the precursor of compound **8**,[43] likewise develops a purple color if allowed to age in solution. A partial loss of NH₃ and hence the formation of *trans*-

[PtCl$_2$(NH$_3$)(1-MeC-*N3*)] and its hydrolysis product **6**, respectively, might account for this observation.

Diplatinum(III) derivative of compound 7

In an attempt to verify the suspected structural similarities between compounds **3a''**, **7**, and **8** (see above and Table 1), aqueous solutions containing compounds **3a''** and **7**, respectively, were treated with NH$_3$. It was anticipated that NH$_3$ would replace the aqua ligands in compounds **3a''** and **7** to give compound **8** in both cases. However, to our surprise, ^{1}H NMR spectroscopy did not reveal formation of compound **8**, and neither did X-ray analysis in case of compound **7**. Rather than substituting the aqua ligand in **7**, the product isolated revealed that oxidation had occurred to a diplatinum(III) complex, *h,t*-[{Pt(NH$_3$)$_2$ (OH)(1-MeC$^-$-*N3,N4*)}$_2$](NO$_3$)$_2$·2[NH$_4$](NO$_3$)·2H$_2$O **(9)**, with the aqua ligands trans to the N4 position of the 1-MeC$^-$ bridges in compound **7** deprotonated to hydoxido ligands and additional ammonia ligands in the two axial positions (Scheme 9).
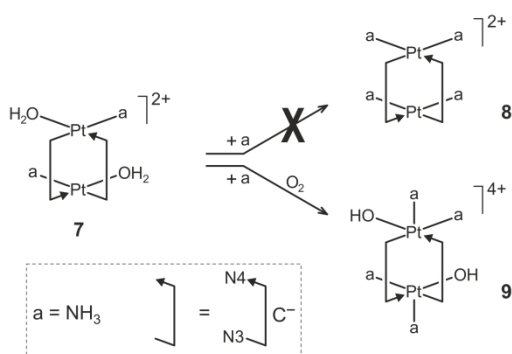
Scheme 9. Reaction of compound **7** with a (a = NH$_3$) in air.

This finding supports the view concerning the ready oxidizability of compound **7**. The ^{1}H NMR spectrum of compound **9** displayed a characteristically downfield shifted H6 doublet (*J* = 7.5 Hz) of 1-MeC$^-$ at *δ* = 7.15 ppm, whereas the H5 doublet (*δ* = 5.78 ppm) and the CH$_3$ singlet (*δ* = 3.31 ppm) were less affected by this reaction. The ^{195}Pt NMR resonance of compound **9** (D$_2$O, *δ* = −638 ppm, singlet) was consistent with a [Pt^{III}]$_2$ structure and the presence of two magnetically equivalent Pt centers. The analogous reaction of compound **3a''** (present in equilibrium with compound **2** and μ-OH complexes) with NH$_3$ likewise yielded a product with its 1-MeC$^-$ resonances at *δ* = 7.16 (d, *J* = 7.5 Hz, H6), 5.77 (d, H5), and 3.31 ppm (s, CH$_3$), which appears to be a diplatinum(III) species.

X-ray crystal structure of compound 9

Figure 12 provides a view of the cation of *h,t*-[{Pt(NH$_3$)$_2$(OH)(1-MeC$^-$-*N3,N4*)}$_2$](NO$_3$)$_2$·2[NH$_4$](NO$_3$)·2 H$_2$O **(9)** and Table 2 lists selected bond distances and angles. Salient structural features are as follows: Both metal ions are hexa-coordinated and are connected by a short Pt–Pt bond. The bond lengths of 2.5406(6) Å

makes it the second shortest bond in diplatinum(III) complexes containing bridging 1-methylcytosinato ligands,[9,41,42] surpassed only by the complex with chelating glycinato ligands at either end of the dinuclear cation.[9] Apart from the Pt–Pt bond lengths, there are several additional differences between compound **9** on one hand and the diplatinum(III) complexes containing equatorial NH$_3$ or ethylenediamine (en) ligands on the other hand. These include the rather small tilt angle of 9.1(2)° between the PtN$_3$O planes in compound **9**, which makes them almost parallel, and the rather modest average torsional angle of 19.5(3)° about the Pt–Pt bond. In complexes containing two NH$_3$ ligands or a chelating en ligand in the plane, tilt angles are ca. 20° or larger, and torsional angles are likewise larger. It appears that intramolecular hydrogen bonding between the OH$^-$ ligand of one Pt plane and the NH$_3$ ligand of the other Pt plane (O12···N13, 2.757(7) Å) in compound **9** is ultimately responsible for these features of cation **9**. Of course, there is only repulsion between NH$_3$ or en ligands in the other mentioned compounds. The geometry of the bridging 1-MeC$^-$ ligand is normal. Specifically, the C4–N4 bond is short (1.305(7) Å), consistent with a pronounced degree of double-bond character. The Pt bonded to the N4 atom is forced out of the plane of the nucleobase (ring atoms N1 to C6, RMSD 0.0382 Å) by −0.581(8) Å, a feature common in diplatinum(III) complexes with 1-methylcytosinato bridges.
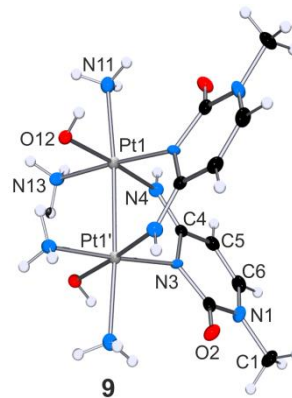
Figure 12. View of cation of compound **9** with atom numbering scheme. Ellipsoids are drawn at the 30% probability level. Symmetry operation to generate the monomer: −x, y, −0.5−z.

Table 2. Selected bond lengths (Å), bond angles (°), and angles between least-squares planes (°) for compound **9**.[a]

Pt1–Pt1'	2.5406(6)	N11–Pt1–Pt1'	176.0(1)
Pt1–N3'	2.061(5)	N13–Pt1–N3'	176.4(2)
Pt1–N4	1.994(5)	N4–Pt1–O12	177.0(2)
Pt1–O12	2.027(4)	N4–Pt1–N13	89.1(2)
Pt1–N13	2.036(5)	N4–Pt1–N3'	91.6(2)
Pt1–N11	2.184(6)	O12–Pt1–N3'	90.2(2)
O12···N13'	2.757(7)	O12–Pt1–N13	89.1(2)
Pt1N$_3$O / Pt1'N$_3$O	9.1(2)	Pt1N3O / 1-MeC	71.7(2)

[a] Symmetry operation for primed atoms: 1 −x, y, −0.5−z

Our initial solution of the crystallographic data of compound **9** was that of a compound of the composition [{Pt(NH$_3$)$_3$(1-MeC-*N3,N4*)}$_2$](NO$_3$)$_4$·4H$_2$O, which has the identical sum formula as the here used one, as supported by the elemental analysis data. It was the unreasonably short intramolecular contacts between the supposed NH$_3$ ligands of the adjacent Pt planes which stirred our doubts, in addition to rather low displacement factors compared to the other non-hydrogen atoms. When replacing one of the NH$_3$ groups trans to the N4 position of 1-MeC$^-$ by OH$_2$, the *R* factor dropped and the displacement factors improved, yet an assumed composition of [{Pt(NH$_3$)$_2$(H$_2$O)$_2$(1-MeC-*N3,N4*)}$_2$](NO$_3$)$_4$·4H$_2$O was at odds with elemental analysis data for N, and common sense tells that a diplatinum aqua complex should likely be formed under acidic conditions only, at least if the aqua ligand is bonded in an equatorial position. Eventually the change of a water ligand into a hydroxido ligand, and recognition that stoichiometric amounts of ammonium nitrate plus sodium hydroxide were applied in the synthesis of compound **9** to generate NH$_3$ (in an attempt to avoid an excess of ammonia), gave the solution used here. This assignment is fully consistent with the X-ray data, and the hydrogen atoms of the hydroxido ligand, the ammonium cation as well as of the additional water of crystallization were located in the difference maps and partially even freely refined (Figure S7 in the Supporting Information).

We note that reaction of compound **7** with NH$_3$ under mild oxidative conditions (presence of air) leads to retention of the original Pt coordination spheres, that is, with the hydroxido ligand staying trans to the N4 atom of the cytosine nucleobases and hence in the plane position rather than moving to the axial position. The situation thus is similar to that seen in the reaction of compound **7** with the amino acid glycine, which also yields a diplatinum(III) product with the carboxylate O atom bonded in plane and the amino group positioned in the apical position.[9] It differs from the situation seen in the asymmetrical diplatinum(III) complex *h,t*-[(H$_2$O)(en)Pt(1-MeC$^-$)$_2$Pt(en)(OH)](ClO$_4$)$_3$,[42] in which one of the two en ligands chelates in a mixed apical/equatorial fashion, with the hydroxido ligand at one of the two Pt ions is trans to the N3 atom of 1-MeC$^-$, however. The water molecule at the second Pt is in axial position.

Complex **7** appears to be an ideal precursor for the formation of oligonuclear diplatinum(III) complexes held together by single or pairwise μ-NH$_2$ bridges following intermolecular condensation reactions between equatorial hydroxido and axial NH$_3$ ligands. Dimer-of-dimer species of this type, containing four Pt^{III} centers and two pairs of bridging α-pyrrolidonato[16b] and acetato[16c] ligands, respectively, have been described. In these cases, intermolecular condensation between axial hydroxide and equatorial ammonia ligands might have led to their formation, hence a variation of the above scenario. We note that during workup of solutions containing compound **7** we

occasionally ended up with highly viscous, yellow-brownish non-crystalline materials, the nature of which has not been established, however.

Mass spectra of solutions containing compound 6

Treatment of *trans*-[PtI$_2$(NH$_3$)(1-MeC-*N3*)] (**5a**) with two equivalents of AgNO$_3$ in water produces the corresponding diaqua species **6**, which, like the corresponding *cis*-isomer **2**, undergoes condensation and Pt oxidation reactions. Representative ESI mass spectra recorded after one and three days of mixing compound **5a** and AgNO$_3$ (and removal of AgI by centrifugation) are provided in Figure S8 in the Supporting Information. Compared to the mass spectra derived from compound **2** (see above), the following similarities and differences were observed: 1) Essentially only singly charged cations are seen. 2) The ambiguity concerning the composition of individual species with regard to tautomerism and possible Pt oxidation state remains. 3) Formation of species beyond the Pt$_2$L$_4$ level (L = 1-MeC$^-$) is not observed with compound **5a**, or at least very much reduced. 4) The tendency of compound **5a** to undergo ligand disproportionation reactions is very pronounced. For example, species of Pt$_1$L$_3$, Pt$_1$L$_2$, Pt$_2$L$_3$, and Pt$_2$L$_4$ stoichiometries are detected, which are formed either in solution or in the gas phase. This finding is in a way reminiscent of similar rearrangement reactions of bis(1-MeC) complexes of *trans*-(NH$_3$)$_2$Pt^{II} occurring in solution.[44] It implies furthermore the formation of Pt species, which no longer carry a nucleobase.

In the following, we will discuss only several selected peak groups in the mass spectra, focussing on the question of Pt oxidation states in these species. First, signals centered around *m/z* = 707 shall be considered (Figure 13). The experimentally obtained spectrum is qualitatively *slightly* different from that obtained with the *cis* isomer (Figure 6) in that the discrepancy in intensities of the *m/z* = 704 peak is too large to be ignored and the signal cannot simply be assigned to the head-tail Pt^{II} dimer [Pt$^{II}_2$(1-MeC$^-$)$_2$(OH$^-$)(NH$_3$)$_2$(H$_2$O)]$^+$ with *m/z* = 707. Rather, it is proposed that the experimental spectrum represents a superposition of *m/z* = 707 and a partially oxidized species with *m/z* = 706, that is, with [Pt^{II}Pt^{III}(1-MeC$^-$)$_2$(OH$^-$)$_2$(NH$_3$)$_2$]$^+$. Second, there are signals grouped at around *m/z* = 860. They are indicative of species of a stoichiometry of Pt$_2$L$_3$, but the number of signal components is too large to assign the experimental spectrum to a single compound (Figure 14). Rather, we propose that it represents a superposition of several (four to five?) sets, ranging from *m/z* = 858 to 862, for example. Possible compositions of four species, differing in the protonation states of ligands (1-MeC or 1-MeC$^-$; H$_2$O or OH$^-$), the Pt oxidation states ([Pt^{II}]$_2$; [Pt^{II}Pt^{III}]; [Pt^{III}]$_2$), as well as the NH$_3$ content, are given in Scheme 10.

There is, in principle, an interesting variant possible to account for the signals with higher *m/z* values (i.e., 861, 862), namely species with Pt oxidation states < 2!

A series of species ranging from $[(Pt^{III})_2(OH)(NH_3)(1\text{-}MeC^-)_3(NO_3)]^+$ (m/z = 858), $[Pt^{III}Pt^{II}(H_2O)(NH_3)(1\text{-}MeC^-)_3(NO_3)]^+$ (m/z = 859), $[(Pt^{II})_2(H_2O)(NH_3)(1\text{-}MeC^-)_2(1\text{-}MeC)(NO_3)]^+$ (m/z = 860), $[Pt^{II}Pt^{I}(H_2O)(NH_3)(1\text{-}MeC^-)(1\text{-}MeC)_2(NO_3)]^+$ (m/z = 861), to $[(Pt^{I})_2(H_2O)(NH_3)(1\text{-}MeC)_3(NO_3)]^+$ (m/z = 862), formed formally in disproportionation reactions $[2\,(Pt^{II})_2 \leftrightharpoons (Pt^{III})_2 + (Pt^{I})_2]$ and subsequent comproportionations $[Pt^{III} + Pt^{II} \rightarrow Pt^{III}Pt^{II};\ Pt^{I} + Pt^{II} \rightarrow Pt^{I}Pt^{II}]$ could account for the presence of five species. Although we do not have any firm evidence for the existence of mixed $Pt^{II}Pt^{I}$ or $(Pt^{I})_2$ complexes, it should be pointed out that reduction of Pt^{II} to Pt^{I} can be achieved under mild conditions in solutions containing water and being exposed to air.[45] Finally, the weak signal set centered around m/z = 925 is even more complex as it represents a superposition of five or even more individual species. The stoichiometry of these species is Pt_2L_4.
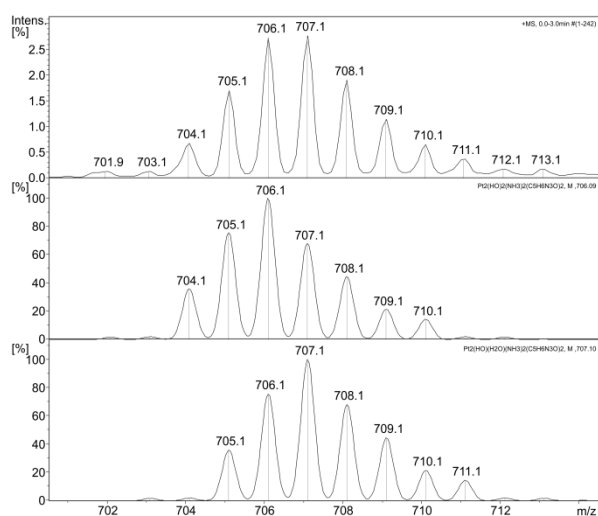

Figure 13. ESI mass spectrum of compound **6** in aqueous solution (top) with simulations for $[Pt_2(1\text{-}MeC^-\text{-}N3,N4)_2(OH)_2(NH_3)_2]^+$ (middle) and $[Pt_2(1\text{-}MeC^-\text{-}N3,N4)(OH)(NH_3)(H_2O)]^+$ (bottom). The Pt concentration was 0.02 M, the target mass was 708.
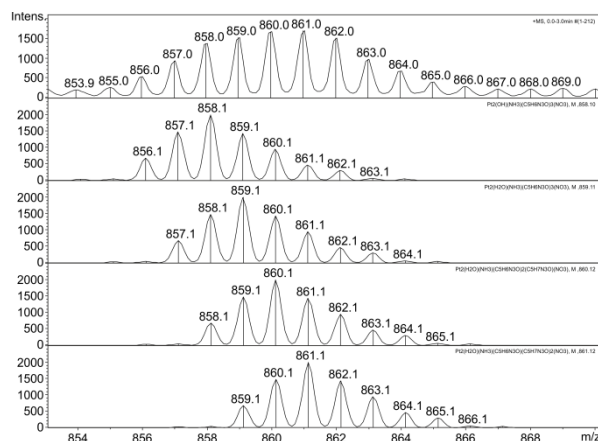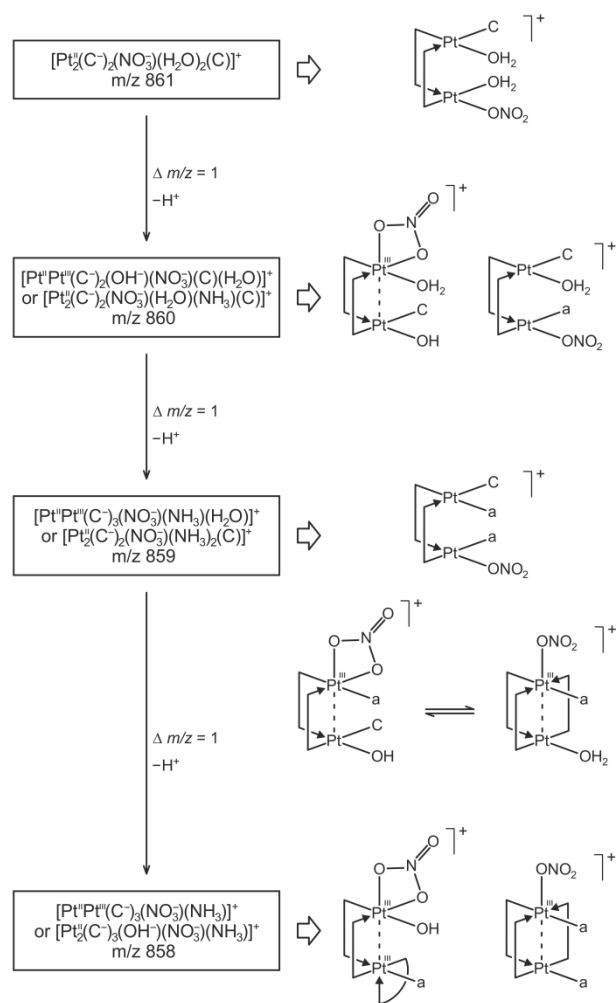

Figure 14. ESI mass spectrum of compound **8** in aqueous solution (top) with simulations for $[Pt_2(1\text{-}MeC^-\text{-}N3,N4)_3(OH)(NH_3)(NO_3)]^+$, $[Pt_2(1\text{-}MeC^-\text{-}N3,N4)_3(H_2O)(NH_3)(NO_3)]^+$, $[Pt_2(1\text{-}MeC^-\text{-}N3)(H_2O)(NH_3)(NO_3)]^+$, and $[Pt_2(1\text{-}MeC^-\text{-}N4)(1\text{-}MeC\text{-}N3)_2(H_2O)(NH_3)(NO_3)]^+$ (second from top to bottom). The Pt concentration was 0.02 M, target mass was 708.

Scheme 10. Proposed decomposition processes based on mixed-valence dinuclear species with m/z = 860 involving loss of single protons combined with a change of oxidation states (stepwise oxidation) of the Pt centers (a = NH_3).

Cytotoxicity testing

Compound **1a** was tested for antiproliferative activity with a crystal violet microtiter assay as described previously[46] against a mini-panel of seven human cancer cell lines: two lung cancer (LCLC-103H and A427), two bladder cancer (5637 and RT-4), one breast cancer (MCF-7), one cervix cancer (SISO) and one pancreas cancer line (DAN-G). Only in the SISO and LCLC-103H lines was appreciable cell growth inhibitory activity observed; that is, with IC_{50} (50% growth inhibitory concentration) values of 4.90 ± 0.91 and 14.90 ± 7.04 µM (mean and standard deviation of three independent experiments), respectively. In all other lines the IC_{50} values were greater than 20 µM. Thus, compound **1a** appears to have selectivity towards cervix cancer. In comparison, cisplatin had much lower IC_{50} values in the same seven cell lines, for example, with values of 0.24 ± 0.06 and 0.90 ± 0.19 µM for the SISO and LCLC-103H cell lines, respectively.[46] However, the selectivity of cisplatin for the SISO line was not as great as that seen with compound **1a**. It would be interesting to now test compound **1a** against

a panel of cervix cancer cell lines to confirm this selectivity.

Conclusion

In the physiological pH range the activated forms of the antitumor agent cisplatin, cis-[Pt(NH$_3$)$_2$(H$_2$O)$_2$]$^{2+}$/cis-[Pt(NH$_3$)$_2$(H$_2$O)(OH)]$^+$, undergo self-condensation reactions in water to give open and cyclic hydroxido-bridged oligomers, unless good nucleophiles are present. The close analogue, cis-[Pt(H$_2$O)$_2$(NH$_3$)(1-MeC-$N3$)]$^{2+}$ (**2**)/cis-[Pt(H$_2$O)(OH)(1-MeC-$N3$)]$^+$, and likewise its isomeric forms $trans$-[Pt(H$_2$O)$_2$(NH$_3$)(1-MeC-$N3$)]$^{2+}$ (**6**)/$trans$-[Pt(H$_2$O)(OH)(1-MeC-$N3$)]$^+$, behave analogously. However, in addition, condensation between a hydroxide ligand and the weakly acidic amino group of the cytosine nucleobase is an alternative, leading to 1-methylcytosinato (1-MeC$^-$-$N3,N4$) bridged species. Although not experimentally observed in the present study, there is even the possibility that an ammonia ligand condenses with a hydroxide ligand to give an amido bridge (μ-NH$_2$).[19] All three condensation patterns require the loss of protons from the original bis(aqua) complex, a feature consistent with the observed drop in the pH value during the ageing process of the diaqua species **2** and **6**. A fourth feasible condensation pattern, leading to (1-MeC-$N3,O2$) bridges, does not involve loss of a proton and is suggested not to play a major role in the aqueous solution chemistry of compounds **2** and **6**, but may be realized in solid-state structures of complexes isolated from acidic solutions.

Regarding 1-metylcytosinato bridged complexes, it is clear that numerous isomers can be formed in principle, yet it appears that dinuclear species with head-tail orientation and cis-arrangement of the two bases are a preferred motif, not only for derivatives of compound **6**, for which structural evidence is available, but probably also for derivatives of compound **2**, according to ^{1}H NMR spectroscopy. The close vicinity of two Pt atoms in these complexes and their orientation relative to each other is favorable for redox processes. UV/vis and EPR spectra clearly suggest the presence of mixed-valence Pt compounds in solution, and the isolation of the new diplatinum(III) compound **9**, obtained without the addition of any oxidizing agent, supports this view.

At the outset of this study it was the hope that by use of ESI mass spectrometry a more detailed analysis of condensation products present in aged solutions of the diaqua complexes **2** and **6** might be obtained. However, these expectations have been met with only partial success. Although the masses of mono-, di-, tri-, and tetranuclear Pt species could be identified, their exact composition in most cases proved ambiguous due to the possibility of proton exchange between different ligands (ligand tautomerism) and the coexistence of oxidized metal species. The MS results revealed, however, extensive ligand disproportionation processes, a feature seen by us occasionally in earlier studies.[44]

Experimental Section

Materials: Cytosine, AgNO$_3$, K$_2$PtCl$_4$, KI, and KBr were of commercial origin and used as received. cis-PtCl$_2$(NH$_3$)$_2$,[47] 1-MeC,[48] cis-[PtCl(NH$_3$)$_2$(1-MeC)]Cl[9], $trans$-PtI$_2$(NH$_3$)(1-MeC-$N3$)[9] and NH$_4$[PtCl$_3$(NH$_3$)][49] were prepared according to literature procedures. 9-EtGH and 1-Et-5-MeC were of commercial origin (Chemogen, Konstanz).

Instrumentation: Elemental analysis data were obtained on a Leco CHNS-932 instrument. The ^{1}H NMR spectra were recorded in D$_2$O ([D$_7$]DMF) on Varian Mercury 200 FT-NMR, Bruker DPX 300, DRX 400 and DRX 500 spectrometers. Chemical shifts D$_2$O are referenced to internal standard sodium-3-(trimethylsilyl)-propane-sulfonate TSP (δ = 0.00 ppm versus tetramethylsilane). [195]Pt NMR shifts were referenced to Na$_2$PtCl$_6$. Spectra recorded in [D$_7$]DMF are referenced to the solvent signal at δ = 8.03 ppm. The pD values of NMR samples in D$_2$O were measured by using a glass electrode and the addition of 0.4 log units to the uncorrected value measured (pH*).

ESI-MS experiments: Aqueous solutions of compounds **1a** and **5** at a concentration of 0.02 M were treated with two equivalents of AgNO$_3$, respectively. The resulting solutions were allowed to age at room temperature. After centrifugation, the supernatants were analyzed by using ESI-MS, carried out with an ESI–quadrupole ion trap instrument (esquire6000, Bruker) with the following settings: Sample flow rate = 4.0 μL/min, nebuliser nitrogen pressure = 689 hPa, spray shield voltage = −3500 kV, capillary entrance voltage = −4000 kV, nitrogen dry gas temperature = 573 K, dry gas flow rate = 5.0 L/min, the helium buffer/collision gas pressure was set to 4.0×10^{-6} hPa (the actual pressure in the analyzer was approximately 100 times higher). Voltages at the capillary exit and lens 2 varied with the change of the target mass.

Preparations of compounds:

cis-PtCl$_2$(NH$_3$)(1-MeC-N3) **(1a):** NH$_4$[Pt(Cl$_3$(NH$_3$)] (200 mg, 0.565 mmol) and 1-MeC (70.6 mg, 0.565 mmol) were dissolved in 4 mL aqueous NaCl solution (c_{NaCl} = 10 M). The solution was stirred for 24 h at 40 °C. The light yellow precipitate formed by then was filtered and washed with water, ethanol, and was subsequently dried at 40 °C. Single crystals were obtained from the filtrate kept at 4 °C for four weeks. Yield: 153 mg (66%); elemental analysis calcd (%) for C$_5$H$_{10}$N$_4$OCl$_2$Pt : C 14.71, H 2.47, N 13.73; found: C 14.7, H 2.5, N 13.8.

cis-PtCl$_2$(NH$_3$)(1-Et-5-MeC-N3) **(1b):** NH$_4$[PtCl$_3$(NH$_3$)] (150 mg, 0.424 mmol) and 1-Et-5-MeC (64.86 mg, 0.424 mmol) were dissolved an aqueous solution of NaCl (3 mL, c_{NaCl} = 2.6 M) each. The solutions were combined and stirred at 40 °C for 4 h. After cooling down to RT the solution was kept at 4 °C overnight. Few single crystals of compound **1b** could be isolated and were identified by X-ray analysis.

$trans$-PtI$_2$(NH$_3$)(1-MeC-N3) **(5):** Compound **5** was prepared according to a literature procedure.[9] Alternatively, compound **5** was obtained by mixing cis-[PtCl(NH$_3$)$_2$(1-MeC-$N3$)]Cl (100 mg, 0.235 mmol) with KI (70.78 mg, 0.47 mmol) in 5 mL of water. The solution was stirred at 40 °C for 3 h and, after cooling to RT, kept at 4 °C. Orange needles of compound **5** formed as a byproduct of cis-[PtI(NH$_3$)$_2$(1-MeC-$N3$)]I and

both products were identified by X-ray analysis (not provided). As crystals of the DMF adduct **5a**, obtained from an NMR sample of compound **5** in DMF solution, proved of better quality than those of compound **5**, only data of compound **5a** is reported. The molecular structures of compounds **5** and **5a** are very similar, however.

trans-[PtBr$_2$(NH$_3$)(1-MeC-N3)] (5b): A suspension of *trans*-PtI$_2$(NH$_3$)(1-MeC-*N3*) (**5**) (100 mg, 0.17 mmol) and AgNO$_3$ (57.48 mg, 0.34 mmol) in water (15 mL) was stirred at RT for 4 h with light excluded. After filtration of the AgI precipitate, KBr (40.27 mg, 0.34 mmol), dissolved in water (1 mL), was added to the filtrate. The dark precipitate which formed immediately, was filtered off and the filtrate was kept at 4 °C for several days until brownish needles of compound **5b** could be isolated. Yield: 24 mg (27.5 %); elemental analysis calcd for C$_5$H$_{12}$N$_4$O$_2$Br$_2$Pt (monohydrate): C 11.69; H 2.35; N 10.92; found: C 11.7; H 2.4; N 11.0.

h,t-[{Pt(NH$_3$)$_2$(OH)(1-MeC$^-$-N3,N4)}$_2$](NO$_3$)$_2$·2[NH$_4$](NO$_3$)·2H$_2$O (9): *trans*-PtI$_2$(NH$_3$)(1-MeC-*N3*) (**5**) (301 mg, 0.5 mmol) was suspended with AgNO$_3$ (169 mg, 1 mmol) in water (20 mL) and the solution was stirred at RT for 4 h. AgI was removed by centrifugation and the solution was adjusted regularly to pH 5 with NaOH for 48 h. NH$_4$NO$_3$ (165 mg, 2.06 mmol) was added and the pH value of the solution was adjusted to approximately 9.5 with NaOH. After 24 h a precipitate of unknown composition was removed by centrifugation. The solution was kept under a gentle stream of nitrogen until the onset of crystallization and then placed in a refrigerator of 4 °C. A mixture of NH$_4$NO$_3$ and yellow compound **9** was then removed and re-crystallized from water. The yield of compound **9** was 41 mg (15 %); elemental analysis calcd for C$_{10}$H$_{38}$N$_{16}$O$_{18}$Pt$_2$: C 11.32; H 3.62; N 21.13; found: C 11.3; H 3.4; N 20.9.

Aqua species of 1a and 5: The aqua species of compounds **1a** and **5** were obtained by mixing either compound **1a** (8.6 mg, 0.02 mmol) or **5** (11.82, 0.02 mmol) with AgNO$_3$ (6.79 mg, 0.04 mmol) in water (1 mL), or for ^{1}H NMR studies in D$_2$O, respectively. The suspensions were stirred over night at RT with light exclusion. The precipitated silver halides were separated by centrifugation.

X-ray crystallography: Intensity were recorded on an Oxford Diffraction Xcalibur S diffractometer (complexes **2a**, **2b**, **5a** and **5b**), and on an Enraf–Nonius KappaCCD (complex **9**) diffractometer, both with graphite monochromated Mo Kα radiation (λ = 0.71073 Å). Data reduction and cell refinement were carried out using the CrysAlisPro software[50] (complexes **2a**, **2b**, **5a**, **5b**), or the DENZO and SCALE-PACK software[51] (complex **9**). The structures were solved by direct or standard Patterson[52] methods and refined by full-matrix least-squares methods based on F^2 by using the SHELXTL PLUS, SHELXL-93, SHELXL-97 and WinGX software.[53] The positions of heavy atoms were deduced from difference Fourier maps and refined anisotropically. In compounds **2a**, **2b**, **5a** and **5b**, protons were included in geometrically calculated positions and refined with isotropic displacement parameters according to the riding model, whereas in compound **9**, the hydrogen atoms of the hydroxido ligand as well as of the ammonia cation and the water molecule of crystallization were located in the difference maps and except for the hydroxide hydrogen refined without restraints.

For the hydroxido ligand the geometry of an idealized OH group was assumed with tetrahedral X–O–H angle and a rotating group refinement applied (command AFIX 147). ISOR restraints were used for the atom C2 in the structure of compound **5b**.

Crystal data for cis-PtCl$_2$(NH$_3$)(1-MeC-N3) (1a): [C$_5$H$_{10}$Cl$_2$N$_4$OPt], M = 408.16 g mol^{-1}, colorless prisms, orthorhombic, space group *Fdd2*, a = 25.8181(10) Å, b = 34.3653(12) Å, c = 4.4503(2) Å, V = 3948.5(3) Å^3, Z = 16, D_{calcd} = 2.746 g cm^{-3}, T = 150(2) K, λ(Mo Kα) = 0.71073 Å, μ = 14.722 mm^{-1}, 13007 reflections collected, 2436 unique (R_{int} = 0.0497), R_1 [I > 2σ(I)] = 0.0219, wR_2 (F, all data) = 0.0396, GoF = 1.074.

Crystal data for cis-PtCl$_2$(NH$_3$)(1-Et-5-MeC-N3)·H$_2$O (1b): [C$_7$H$_{16}$Cl$_2$N$_4$O$_2$Pt], M = 454.23 g mol^{-1}, colorless prisms, orthorhombic, space group *Pbca*, a = 7.3380(7) Å, b = 19.1423(7) Å, c = 19.3797(10) Å, V = 2722.2(3) Å^3, Z = 8, D_{calcd} = 2.217 g cm^{-3}, T = 150(2) K, λ(Mo Kα) = 0.71073 Å, μ = 10.694 mm^{-1}, 8382 reflections collected, 2998 unique (R_{int} = 0.0276), R_1 [I > 2σ(I)] = 0.0289, wR_2 (F, all data) = 0.0629, GoF = 0.944.

Crystal data for trans-[PtI$_2$(NH$_3$)(1-MeC-N3)]·DMF (5a): [C$_8$H$_{17}$I$_2$N$_5$O$_2$Pt], M = 664.16 g mol^{-1}, yellow needles, triclinic, space group *P–1*, a = 6.8772(6) Å, b = 8.3733(6) Å, c = 14.0948(10) Å, α = 75.203(6)°, β = 84.471(6)°, γ = 84.057(6)°, V = 778.46(10) Å^3, Z = 2, D_{calcd} = 2.833 g cm^{-3}, T = 150(2) K, λ(Mo Kα) = 0.71073 Å, μ = 12.981 mm^{-1}, 5717 reflections collected, 3556 unique (R_{int} = 0.0347), R_1 [I > 2σ(I)] = 0.0319, wR_2 (F, all data) = 0.0583, GoF = 0.990.

Crystal data for trans-[PtBr$_2$(NH$_3$)(1-MeC-N3)] (5b): [C$_5$H$_{10}$Br$_2$N$_4$OPt], M = 497.08 g mol^{-1}, orange blocks, monoclinic, space group *P21/c*, a = 6.7429(8) Å, b = 20.2180(19) Å, c = 8.6316(10) Å, β = 110.205(14)°, V = 1104.3(2) Å^3, Z = 4, D_{calcd} = 2.990 g cm^{-3}, T = 150(2) K, λ(Mo Kα) = 0.71073 Å, μ = 19.913 mm^{-1}, 7654 reflections collected, 2523 unique (R_{int} = 0.0571), R_1 [I > 2σ(I)] = 0.0350, wR_2 (F, all data) = 0.0580, GoF = 0.849.

Crystal data for h,t-[{Pt(NH$_3$)$_2$(OH)(1-MeC$^-$-N3,N4)}$_2$](NO$_3$)$_2$·2[NH$_4$](NO$_3$)·2H$_2$O (9): [C$_{10}$H$_{38}$N$_{16}$O$_{18}$Pt$_2$], M = 1060.74 g mol^{-1}, brown blocks, monoclinic, space group *C2/c*, a = 17.174(3) Å, b = 19.440(4) Å, c = 10.551(2) Å, β = 118.51(3)°, V = 3095.4(10) Å^3, Z = 4, D_{calcd} = 2.276 g cm^{-3}, T = 183(2) K, λ(Mo Kα) = 0.71073 Å, μ = 9.128 mm^{-1}, 10682 reflections collected, 2801 unique (R_{int} = 0.0957), R_1 [I > 2σ(I)] = 0.0297, wR_2 (F, all data) = 0.0698, GoF = 1.003.

CCDC-1401095 (**1a**), -1401096 (**1b**), -1401097 (**5a**), -1401098 (**5b**), and -1400366 (**9**) contain the supplementary crystallographic data for this paper. These data can be obtained free of charge from The Cambridge Crystallographic Data Centre via www.ccdc.cam.ac.uk/data_request/cif.

Acknowledgements

References

[1] a) Various articles in *Platinum Coordination Complexes in Cancer Chemotherapy* (Eds.: T. A. Connors, J. J. Roberts, Springer, Berlin, **1974**; b) A. J. Thomson, R. J. P. Williams, S. Reslova, *Struct. Bonding* **1972**, *11*, 1-46; c) M. J. Cleare, J. D. Hoeschele, *Bioinorg. Chem.* **1972**, *2*, 187–210.

[2] See, e.g.: a) M. van Beusichen, N. Farrell, *Inorg. Chem.* **1992**, *31*, 634–639; b) M. Coluccia, A. Nassi, F. Loseto, A. Boccarelli, M. A. Mariggio, D. Giordano, F. P. Intini, P. Caputo, G. Natile, *J. Med. Chem.* **1993**, *36*, 510–512; c) E. I. Montero, S. Diaz, A. M. Gonzalez-Vadillo, J. M. Perez, C. Alonso, C. Navarro-Ranninger, *J. Med. Chem.* **1999**, *42*, 4264–4268; d) J. B. Mangrum, N. P. Farrell *Chem. Commun.* **2010**, *46*, 6640–6650; e) T. C. Johnstone, J. J. Wilson, S. J. Lippard, *Inorg. Chem.* **2013**, *52*, 12234–12249, and references therein.

[3] L. R. Kelland, in *Cisplatin—Chemistry and Biochemistry of a Leading Anticancer Drug* (Ed.: B. Lippert), HVCA/Wiley-VCH, Zürich/ Weinheim, **1999**, 497–521.

[4] a) U. Bierbach, Y. Qu, T. W. Hambley, J. Peroutka, H. L. Nguyen, M. Doedee, N. Farrell, *Inorg. Chem.* **1999**, *38*, 3535–3542; b) G. McGowan, S. Parsons, P. J. Sadler, *Inorg. Chem.* **2005**, *44*, 7459–7467.

[5] a) L. S. Hollis, A. R. Amundsen, E. W. Stern, *J. Med. Chem.* **1989**, *32*, 128–136; b) S. F. Bellon, S. J. Lippard, *Biophys. Chem.* **1990**, *35*, 179–188; c) E. L. M. Lempers, M. J. Bloemink, J. Brouwer, Y. Kidani, J. Reedijk, *J. Inorg. Biochem.* **1990**, *40*, 23–35; d) N. Margiotta, G. Natile, F. Capitelli, F. P. Fanizzi, A. Boccarelli, P. De Rinaldis, D. Giordano, M. Coluccia, *J. Inorg. Biochem.* **2006**, *100*, 1849–1857; e) T. C. Johnstone, S. J. Lippard, *J. Am. Chem. Soc.* **2014**, *136*, 2126–2134.

[6] Y. Chen, Z. Guo, S. Parsons, P. J. Sadler, *Chem. Eur. J.* **1998**, *4*, 672–676.

[7] a) D. Wang, G. Zhu, X. Huang, S. J. Lippard, *Proc. Natl. Acad. Sci. USA* **2010**, *107*, 9584–9589; b) K. S. Lovejoy, R. C. Todd, S. Zhang, M. S. McCormick, J. A. D'Aquino, J. T. Reardon, A. Sancar, K. M. Giacomini, S. J. Lippard, *Proc. Natl. Acad. Sci. USA* **2008**, *105*, 8902–8907; c) C. Bauer, T. Peleg-Shulman, D. Gibson, A. H.-J. Wang, *Eur. J. Biochem.* **1998**, *256*, 253–260.

[8] See, e.g.: a) P. M. Lax, M. Garijo Añorbe, B. Müller, E. Y. Bivián-Castro, B. Lippert, *Inorg.Chem.* **2007**, *46*, 4036–4043; b) A. Galstyan, W.-Z. Shen, B. Lippert, *Z. Naturforsch.* **2009**, *46b*, 1653–1661; c) B. Lippert, *Chem. Biodiversity* **2008**, *5*, 1455–1474.

[9] T. Wienkötter, M. Sabat, G. Fusch, B. Lippert, *Inorg. Chem.* **1995**, *34*, 1022–1029.

[10] B. Lippert, *Prog. Inorg. Chem.* **1989**, *37*, 1–97.

[11] a) R. Faggiani, C. J. Lock, B. Lippert, *Inorg. Chim. Acta* **1985**, *106*, 75–79; b) E. Freisinger, A. Schneider, M. Drumm, A. Hegmans, S. Meier, B. Lippert, *J. Chem. Soc. Dalton Trans.* **2000**, 3281–3287; c) E. Freisinger, S. Meier, B. Lippert *J. Chem. Soc. Dalton Trans.* **2000**, 3274–3280; d) A. Hegmans, M. Sabat, I. Baxter, E. Freisinger, B. Lippert, *Inorg. Chem.* **1998**, *37*, 4921–4928.

[12] a) P. J. Sanz Miguel, M. Roitzsch, L. Yin, P. M. Lax, L. Holland, O. Krizanovic, M. Lutterbeck, M. Schürmann, E. C. Fusch, B. Lippert *Dalton Trans.* **2009**, 10774–10786; b)

[12] M. Krumm, I. Mutikainen, B. Lippert, *Inorg. Chem.* **1991**, *30*, 884–890.

[13] Following the pD dependence of the $^{15}NH_3$ resonance in *cis*-[Pt(H$_2$O)$_2$(^{15}NH$_3$)X]$^+$, two individual pK_a values of aqua ligands of 5.22 and 7.16 (X = 3-picoline) were reported by Sadler *et al.* (Ref. [6]). Conditions were 3mM in c$_{Pt}$ and 100 mM NaClO$_4$. With a structurally related complex, i.e., X = 2-(2-hydroxyethylpridine), for the two deprotonation steps (pK_a = 3.90 and 4.78) the second pK_a value is remarkably low: A. C. G. Hotze, Y. Chen, T. W. Hambley, S. Parsons, N. A. Kratochwil, J. A. Parkinson, V. P. Muntz, P. J. Sadler, *Eur. J. Inorg. Chem.* **2002**, 1035–1039.

[14] R. B. Martin in *Cisplatin—Chemistry and Biochemistry of a Leading Anticancer Drug* (Ed.: B. Lippert), HVCA Zürich and Wiley-VCH Weinheim, **1999**, 183–205.

[15] For μ-OH complexes of *cis*-a$_2$Pt^{II}, see: a) R. Faggiani, B. Lippert, C. J. L. Lock, B. Rosenberg, *J. Am. Chem. Soc.* **1977**, *99*, 777–781; b) R. Faggiani, B. Lippert, C. J. L. Lock, B. Rosenberg, *Inorg. Chem.* **1977**, *16*, 1192–1196; c) R. Faggiani, B. Lippert, C. J. L. Lock, B. Rosenberg, *Inorg. Chem.* **1978**, *17*, 1941–1945; d) J. A. Stanko, L. S. Hollis, J. A. Schreifels, J. D. Hoeschele, *J. Clin. Hemat. Oncol.* **1977**, *7*, 138–168; e) J.-P. Macquet, S. Cros, A. L. Beauchamp, *J. Inorg. Biochem.* **1985**, *25*, 197–206; f) F. D. Rochon, A. Morneau, R. Melanson, *Inorg. Chem.* **1988**, *27*, 10–13.

[16] a) L. Heck, M. Ardon, A. Bino, J. Zapp, *J. Am. Chem. Soc.* **1988**, *110*, 2691-2692; b) K. Matsumoto, K. Harashima, *Inorg. Chem.* **1991**, *30*, 3032–3034; c) J. Wilson, S. J. Lippard, *Inorg. Chem.* **2012**, *51*, 9852–9864.

[17] N. W. Alcock, P. Bergamini, T. J. Kemp, P. G. Pringle, S. Sostero, O. Traverso, *Inorg. Chem.* **1991**, *30*, 1594–1598.

[18] G. Kampf, P. J. Sanz Miguel, M. Morell Cerdà, M. Willermann, A. Schneider, B. Lippert, *Chem. Eur. J.* **2008**, *14*, 6882–6891.

[19] L. Yin, M. Sodupe, L. Rodríguez-Santiago, P. J. Sanz Miguel, B. Lippert, to be published.

[20] a) T. J. Kistenmacher, M. Rossi, L. G. Marzilli, *Inorg. Chem.* **1979**, *18*, 240–244; b) P. Amo-Ochoa, O. Castillo, P. J. Sanz Miguel, F. Zamora, *J. Inorg. Biochem.* **2008**, *102*, 203–208; c) B. Lippert, U. Thewalt, H. Schöllhorn, D. M. L. Goodgame, R. W. Rollins, *Inorg. Chem.* **1984**, *23*, 2807–2813; d) H. Schöllhorn, U. Thewalt, B. Lippert, *Inorg. Chim. Acta* **1987**, *135*, 155–159.

[21] a) F. Pichierri, D. Holthenrich, E. Zangrando, B. Lippert, L. Randaccio, *J. Biol Inorg. Chem.* **1996**, *1*, 439–445; b) J. Müller, E. Zangrando, N. Pahlke, E. Freisinger, L. Randaccio, B. Lippert *Chem. Eur. J.* **1998**, *4*, 397–405; c) J. Müller, F. Glahé, E. Freisinger, B. Lippert *Inorg. Chem.* **1999**, *38*, 3160–3166.

[22] In weakly acidic medium the N4 coordinated 1-MeC is likely to exist in its imino tautomer structure, with N3 carrying a proton.

[23] B. Lippert in *Cisplatin—Chemistry and Biochemistry of a Leading Anticancer Drug* (Ed.: B. Lippert), HVCA/Wiley-VCH, Zürich/ Weinheim, **1999**, 379–404.

[24] a) P. Zaplatynski, H. Neubacher, W. Lohmann, *Z. Naturforsch.* **1979**, *34b*, 1466–1467; b) H. Neubacher, J. Kieger, P. Zaplatynski, W. Lohmann, *Z. Naturforsch.* **1982**, *37b*, 790–792.

[25] S. Siebel, C. Dammann, W. Hiller, T. Drewello, B. Lippert, *Inorg. Chim. Acta* **2012**, 393, 212–221.

[26] B. Lippert, H. Schöllhorn, U. Thewalt, *Inorg. Chem.* **1986**, *25*, 407–408.

[27] a) M. Authier-Martin, A. L. Beauchamp, *Can. J. Chem.* **1977**, *55*, 1213–1217; b) C. Gagnon, A. L. Beauchamp, D. Tranqui, *Can. J. Chem.* **1979**, *57*, 1372–1376; c) O. Renn, H. Preut, B. Lippert, *Inorg. Chim. Acta* **1991**, *188*, 133–137.

[28] H. Schöllhorn, R. Beyerle-Pfnür, U. Thewalt, B. Lippert, *J. Am. Chem. Soc.* **1986**, *108*, 3680–3688.

[29] W.-Z. Shen, D. Gupta, B. Lippert, *Inorg. Chem.* **2005**, *44*, 8249–8258.

[30] L. Schenetti, G. Bandoli, U. Casellato, B. Corrain, M. Nicolini, B. Longato, *Inorg. Chem.* **1994**, *33*, 3169–3176.

[31] L. Yin, P. J. Sanz Miguel, W.-Z. Shen, B. Lippert, *Chem. Eur. J.* **2009**, *15*, 10723–10726.

[32] Stereochemical descriptors of square planar complexes SP-4 are derived by application of the priority rule, which is Cl > 1-MeC-*N3* > G-*N7* > NH$_3$. The number "N" in SP-4-N refers to the priority of the ligand trans to the ligand of highest priority, which is Cl$^-$. If NH$_3$ is trans to Cl, the description is SP-4-4, for example.

[33] M. C. Biagini, M. Ferrari, M. Lanfranchi, L. Marchiò, M. A. Pellinghelli, *J. Chem. Soc. Dalton Trans.* **1999**, 1575–1580.

[34] P. M. Takahara, A. C. Rosenzweig, C. A. Frederick, S. J. Lippard, *Nature*, **1995**, *377*, 649–652.

[35] G. McGowan, S. Parsons, P. J. Sadler, *Chem. Eur. J.* **2005**, *11,* 4396–4404.

[36] A. Erxleben, S. Metzger, J. F. Britten, C. J. L. Lock, A. Albinati, B. Lippert. *Inorg. Chim. Acta* **2002**, *339*, 461–469.

[37] B. Lippert, *J. Am. Chem. Soc.* **1981,** *103*, 5691–5697.

[38] B. Lippert, *Inorg. Chim. Acta* **1981**, *56*, L23–L24.

[39] B. Lippert, C. J. L. Lock, R. A. Speranzini, *Inorg. Chem.* **1981**, *20*, 808–813.

[40] T. Wienkötter, M. Sabat, G. Trötscher-Kaus, B. Lippert, *Inorg. Chim. Acta* **1997**, *255*, 361–366.

[41] a) R. Faggiani, B. Lippert, C. J. L. Lock, R. A. Speranzini, *J. Am. Chem. Soc.* **1981**, 1111–1120; for a correction, see reference [26] in reference [9]; b) G. Kampf, M. Willermann, E. Zangrando, L. Randaccio, B. Lippert, *Chem. Commun.* **2001**, 747–748; c) G. Kampf, M. Willermann, E. Freisinger, B. Lippert, *Inorg. Chim. Acta* **2002**, *330*, 179–188.

[42] For related (en)Pt complexes, see: V. M. Djinovic, M Galanski, V. B. Arion, B. K. Keppler, *Dalton. Trans.* **2010**, *39*, 3633–3643.

[43] B. Lippert, C. J. L. Lock, R. A. Speranzini, *Inorg. Chem.* **1981**, *20*, 335–342.

[44] a) J. Müller, E. Freisinger, P. J. Sanz Miguel, B. Lippert, *Inorg. Chem.* **2003**, *45*, 5117–5125; b) O. Krizanovic, F. J. Pesch, B. Lippert, *Inorg. Chim. Acta* **1989**, *165*, 145–146.

[45] P. Betz, A. Bino, *J. Am. Chem. Soc.* **1998**, *110,* 602–603.

[46] K. Bracht, Boubakari, R. Grünert, P.J. Bednarski *Anti-Cancer Drugs* **2006**, *17*, 41–51.

[47] G. Raudaschl, B. Lippert, J. D. Hoeschele, H. E. Howard-Lock, C. J. L. Lock, P. Pilon, *Inorg. Chim. Acta* **1985**, *106*, 141–149.

[48] T. J. Kistenmacher, M. Rossi, J. P. Caradonna, L. G. Marzilli, *Adv. Mol. Rel. Interact. Processes* **1979**, *15*, 119–133.

[49] A. Oksanen, M. Leskelä, *Acta Chem. Scand.* **1994**, *48*, 485–489.

[50] CrysAlisPro, Oxford Diffraction (Poland), **2010**.

[51] Z. Otwinowsky, W. Minor, *Methods Enzymol.* **1997**, *276*, 307–325.

[52] G. M. Sheldrick, *Acta Crystallogr. Sect. A* **1990**, 46, 467–473.

[53] a) SHELXTL PLUS (VMS), G. M. Sheldrick, Siemens Analytical X-Ray Instruments, Inc., Madison, WI, **1990**; b) SHELXL-93, Program for Crystal Structure Refinement, G. M. Sheldrick, University of Göttingen (Germany), **1993**; c) SHELXS-97 and SHELXL-97, G. M. Sheldrick, University of Göttingen (Germany), **1997**; d) WinGX, L. J. Farrugia, University of Glasgow (Great Britain), **1998**.

Table of Contents
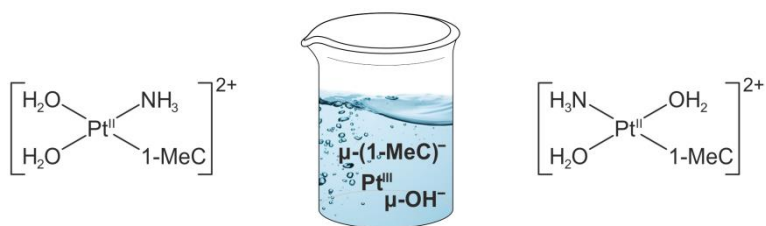
A question of coordination: Multiple self-condensation reactions involving water and 1-methylcytosine (1-MeC) ligands, as well as ready metal oxidation dominate the aqueous solution chemistry of mononuclear *cis-* and *trans-* [Pt(H$_2$O)$_2$(NH$_3$)(1-MeC-*N3*)]$^{2+}$, analogues of the diaqua species of cisplatin and its trans isomer, respectively (see scheme).